N[illegible]A CON[illegible]ACTOR
REP[illegible]T

NASA CR-936

NASA CR-936

D[illegible]NAMIC S[illegible]BILITY O[illegible] SPACE V[illegible]ICLES

Vo[illegible]me II - Deter[illegible]ation of Lo[illegible]itudinal Vib[illegible]n Modes

b[illegible] A. Staley

P[illegible]d by
G[illegible]AL DYNAMIC[illegible]PORATION
S[illegible]go, Calif.
fo[illegible]ge C. Marshall [illegible]ht Center

NA[illegible]AL AERONAUTICS [illegible]ACE ADMIN[illegible]

[redacted]

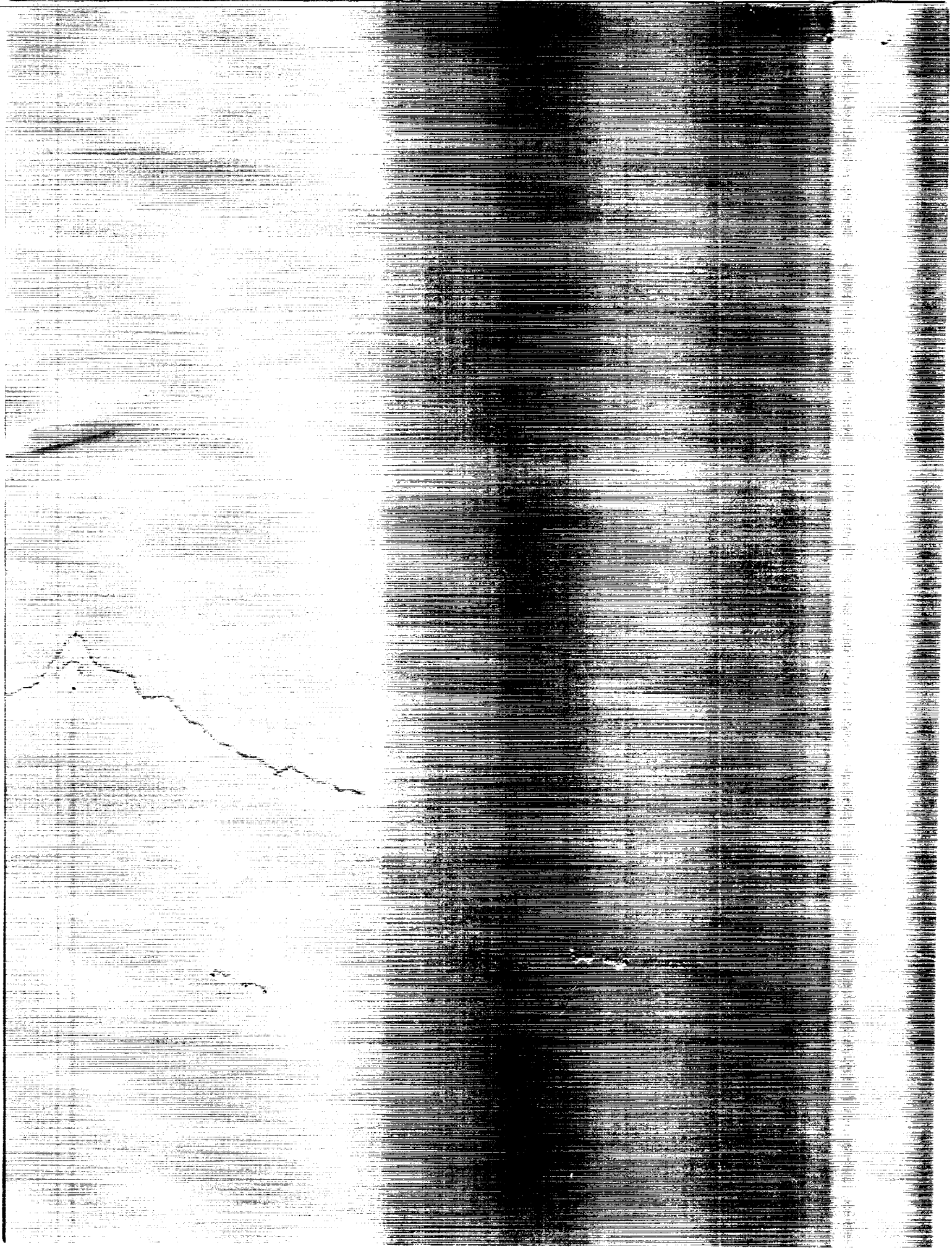

NASA CR-936

DYNAMIC STABILITY OF SPACE VEHICLES

Volume II - Determination of Longitudinal Vibration Modes

By J. A. Staley

Issued by Originator as Report No. GDC-BTD67-053

Prepared under Contract No. NAS 8-11486 by
GENERAL DYNAMICS CORPORATION
San Diego, Calif.

for George C. Marshall Space Flight Center

NATIONAL AERONAUTICS AND SPACE ADMINISTRATION

For sale by the Clearinghouse for Federal Scientific and Technical Information
Springfield, Virginia 22151 – CFSTI price $3.00

FOREWORD

This report is one of a series in the field of structural dynamics prepared under contract NAS 8-11486. The series of reports is intended to illustrate methods used to determine parameters required for the design and analysis of flight control systems of space vehicles. Below is a complete list of the reports of the series.

Volume I	Lateral Vibration Modes
Volume II	Determination of Longitudinal Vibration Modes
Volume III	Torsional Vibration Modes
Volume IV	Full Scale Testing for Flight Control Parameters
Volume V	Impedence Testing for Flight Control Parameters
Volume VI	Full Scale Dynamic Testing for Mode Determination
Volume VII	The Dynamics of Liquids in Fixed and Moving Containers
Volume VIII	Atmospheric Disturbances that Affect Flight Control Analysis
Volume IX	The Effect of Liftoff Dynamics on Launch Vehicle Stability and Control
Volume X	Exit Stability
Volume XI	Entry Disturbance and Control
Volume XII	Re-entry Vehicle Landing Ability and Control
Volume XIII	Aerodynamic Model Tests for Control Parameters Determination
Volume XIV	Testing for Booster Propellant Sloshing Parameters
Volume XV	Shell Dynamics with Special Applications to Control Problems

The work was conducted under the direction of Clyde D. Baker and George F. McDonough, Aero Astro Dynamics Laboratory, George C. Marshall Space Flight Center. The General Dynamics Convair Program was conducted under the direction of David R. Lukens.

TABLE OF CONTENTS

		Page
1	INTRODUCTION	1
2	STATE OF THE ART	3
	2.1 Liquid Propellant Vehicles	3
	2.2 Solid Propellant Vehicles	4
3	MODEL REQUIREMENTS AND RECOMMENDED PROCEDURES	5
	3.1 Liquid-Propellant Vehicle	9
	3.1.1 Selection of Masses	9
	3.1.2 Liquid Propellant and Tank Representation: Spring-Mass Models	10
	3.1.2.1 Basic Single-Mass Model	13
	3.1.2.2 Spring Rates for Tank Bottoms	19
	3.1.2.3 Tanks with Stringers and Buckled Skin	20
	3.1.2.4 Effects of Small Ullage Volumes	22
	3.1.2.5 Multimass Models	28
	3.1.2.6 Tanks with Conical Sections	33
	3.1.3 Local Structure Effects	41
	3.1.4 Temperature	41
	3.1.5 Effect of Axial Load on Stiffness of Skin-Stringer Structures	41
	3.1.6 Improved Analytical Analysis	41
	3.2 Adding Components Using Mode Synthesis	44
	3.3 Correcting Model Based on Test Results	45
	3.4 Solid-Propellant Boosters	46
	3.5 Clustered Boosters	47
	3.6 Lateral-Torsional-Longitudinal Coupling	49
	3.7 Damping Effects	50
4	METHODS FOR SOLUTION	51
	4.1 Formation of the Equations for Solution	51
	4.1.1 Stiffness Matrix	51
	4.1.2 Flexibility Matrix	54
	4.1.3 Transformed Mass Matrix	54
	4.2 Solution for Characteristics	55
	4.3 Modal Synthesis	56
5	REFERENCES	57

LIST OF ILLUSTRATIONS

		Page
1	Two-Degree-of-Freedom System	5
2	Cylindrical Tank and Liquid	11
3	Partially Filled Tank	13
4	Tank Strains	14
5	Equivalent Tank Model	14
6	Variation of $F(f,\nu)$ with Depth-to-Radius Ratio for Various Values of Poisson's Ratio	20
7	Variation of $G(f,\nu)$ with Depth-to-Radius Ratio for Various Values of Poisson's Ratio	20
8	Variation of $H(f,\nu)$ with Depth-to-Radius Ratio for Various Values of Poisson's Ratio	20
9	Skin-Stringer Cylinder Tank Model	21
10	Skin-Stringer Model with Buckled Skin	22
11	Tank with Small Ullage Volume	25
12	Tank Model for Small Ullage Volume	28
13	Two-Element Tank	29
14	Assumed Forces on Two-Element Tank	30
15	Two-Mass Tank Model	32
16	Vehicle with Cone-Cylinder Tank	33
17	Cone-Cylinder Tank	34
18	Equivalent Cylinder Model	35
19	Two-Mass Cone-Cylinder Model	36
20	Radial Deformations in Two-Mass Cone-Cylinder Model	36
21	Natural Frequency of Cone-Cylinder Tank	40
22	Vehicle and Idealization in Basic Components	42
23	Solid-Propellant Rocket Element	46
24	Titan IIIC	48

LIST OF ILLUSTRATIONS (Continued)

		Page
25	Spring-Mass Model	51
26	Model Corresponding to Stiffness Matrix	52

1/INTRODUCTION

This monograph discusses elastic longitudinal models of space launch vehicles and methods used to determine the dynamic characteristics needed for analysis of vehicle response and stability. The types of vehicles considered are multistage liquid and solid propellant vehicles and vehicles with clustered tanks. Longitudinal dynamics have been uncoupled from lateral and torsional dynamics in the frequency range of interest for most launch vehicle systems studied to date; however, such coupling can be important for spacecraft as well as for launch vehicles with the proper characteristics.

The basic method of analysis of longitudinal dynamics problems is to formulate a mathematical model for the vehicle, establishing mass and stiffness model properties from corresponding vehicle properties. Normal modes of the model are then determined, and the response to a particular excitation is found from the normal mode and excitation properties. This method closely parallels that for lateral dynamics.

Since analyses are made using properties of the model, the results are only as good as the model. The model requirements depend on the particular problem being studied and the desired results. Simplifying assumptions are usually made in idealizing the vehicle, so that only significant dynamic phenomena are represented; usually only the lowest frequency modes of the vehicle are of interest. To a great extent, judgment requiring some experience and understanding of the vehicle structural components must be used in developing a simple but adequate vehicle model.

The most significant masses involved in launch vehicle longitudinal dynamics are the propellant masses; other important masses related to the vehicle lower frequency modes are usually the remaining heavier masses such as payload and engines. The significant structural elements are propellant tanks, interstage adapters, and tank bulkheads. Vehicles are usually symmetric about their longitudinal axes, and this permits the use of what is effectively a one-dimensional model.

The propellant mass varies slowly with time in the particular stage that is burning. This permits the assumption that the mass is constant at any particular instant of time. Analysis on this basis is usually referred to as the time-slice approach and is adequate for most problems.

The most significant stiffnesses are usually related to the propellant tanks, interstage structures, and engine supports. Stiffnesses related to propellant tanks vary with time since the basic configuration of the vehicle is changing as propellants are consumed.

For liquid propellant launch vehicles with thin-skinned cylindrical tanks, lumped-mass models are adequate for determination of the lowest vehicle modal properties. For vehicles with more complex tank geometries, more general methods such

as the use of finite shell elements to construct a vehicle model may be required. Models of solid-propellant rockets may be obtained by either continuous representation of the core and casing or by making a simple model that takes into account the mass and shear stiffness of the solid propellant core.

The problems to be analyzed using longitudinal models include response to engine ignition and shutdown transients, release of a vehicle from its launcher, and the stability of engine-structure coupled oscillations. A second stability problem peculiar to liquid-propellant vehicles with thin-skinned tanks involves coupling between structural motions and the tank pressure regulation system. Each of these problems may require different emphasis on details of the model used.

2/STATE OF THE ART

The analysis of liquid- and solid-propellant vehicle longitudinal dynamics may be discussed separately since the modeling problems are of a different nature for the two types of vehicles.

2.1 LIQUID-PROPELLANT VEHICLES

The unique problem in liquid-propellant vehicles is representation of liquid-propellant tanks. The longitudinal dynamics of elastic tanks containing liquid propellants have been analyzed in considerable detail; for example, Reference 1. The types of tanks that have generally been considered are axisymmetric. Effects that have been considered include tank initial stresses, liquid surface waves (sloshing), tank surface motions that are not symmetric, compressibility of ullage gas, elastic effects of bulkheads, and orthotropic tank construction. Analyses including many of these effects are very complex; as a result, use of such analyses in developing a vehicle model has been limited.

The tank models used extensively to study vehicle longitudinal dynamics have generally included a simplified representation of the tank longitudinal dynamics. Reference 2, for example, presents various single-degree-of-freedom models for longitudinal vibration analysis of liquid-propellant cylindrical tanks. These single-degree-of-freedom models were derived based on the assumption that the liquid has a longitudinal acceleration (relative to the tank bottom) that is constant from the liquid surface to the bottom of the tank. Liquid motion is due to tank wall and tank bottom radial and longitudinal deformations. These deformations per unit inertial force of the liquid provide information that can be used to develop a model for the tank. Reference 3 uses a similar tank model to study the coupling between vehicle longitudinal oscillations and propellant tank pressure regulation at launch for an Atlas vehicle. Reference 4 indicates how to include the effective stiffnesses of bulkheads forming tank bottoms for cylindrical tanks. Extension of the single-degree-of-freedom spring-mass model to include higher degrees of freedom is also discussed in Reference 3.

Simple models for other commonly used tank shapes, such as ellipsoidal tanks and tanks with conical sections, may be derived in a manner similar to models derived for cylindrical tanks, but the problem is somewhat more difficult.

A recently developed method of liquid tank representation is presented in Reference 5. A finite element representation of tank and other vehicle components is used to develop the vehicle stiffness matrix; the vehicle is divided into axisymmetric shell components. Fluid motions are assumed to be consistent with the shell component distortions while fluid sloshing effects are neglected. The vehicle stiffness

and mass matrices are obtained by superposition of matrices of individual elements. Only axisymmetric shell motions are considered. Each tank may be composed of ellipsoidal, conical, and cylindrical elements. This model may include higher modes of the tank, bulkhead effects, and general shapes of tanks.

Effects not included in the simpler spring-mass models or the model of Reference 5 are tank motions that are not axisymmetric, i.e., motions that vary around the tank circumference and the effects of fluid surface motion.

The vehicle mass and stiffness matrices that result from use of the tank models discussed may be operated on using standard techniques to determine the vehicle natural frequency and natural mode properties to be used in longitudinal response analyses.

The stiffness of a local structure may be evaluated by use of finite elements to develop stiffness matrices by methods such as that presented in Reference 6. Local structure stiffness should also be verified by tests where possible.

2.2 SOLID-PROPELLANT VEHICLES

Solid-propellant rockets have generally been represented by continuous models. Reference 7 provides a detailed analysis of the structural dynamics of a solid rocket. It includes a discussion of propellant stress-strain properties and analysis of several problems using a continuous representation. The effective longitudinal stiffness of the solid rocket depends primarily on the solid-propellant longitudinal shear stiffness since inertial forces acting on the core material are transmitted to the rocket casing through shear stresses developed in the core material. The rocket casing may be relatively stiff longitudinally in comparison to the core; in this instance the simplifying assumption of a rigid casing might be made.

The remainder of the vehicle, adapters, payload, etc., may be modeled in the same manner as discussed for the liquid-propellant vehicle.

3/MODEL REQUIREMENTS AND RECOMMENDED PROCEDURES

The problem of determining the response of a structure to a particular forcing function consists of formulating the equations of motion for the structure and obtaining a solution to these equations. The solution is usually easier to obtain if the equations of motion are written in terms of the vehicle normal mode coordinates. The use of matrix notation also permits simplified discussion of the general analytical problem and provides a compact format for organizing data for computations.

Natural modes and frequencies may be determined from equations of motion of a system with external forces equal to zero. The equations of motion may be derived from considerations of dynamic equilibrium or by use of energy concepts and LaGrange's equation. As a simple example of the use of equilibrium to derive the equations of motion, consider the two-degree-of-freedom system of Figure 1. The symbols m and K represent masses and spring rates, x represents displacement, and subscripts 1, 2, and 3 refer to nodes of the structure. Masses are lumped at these nodes, and massless springs connect the nodes in this particular example.

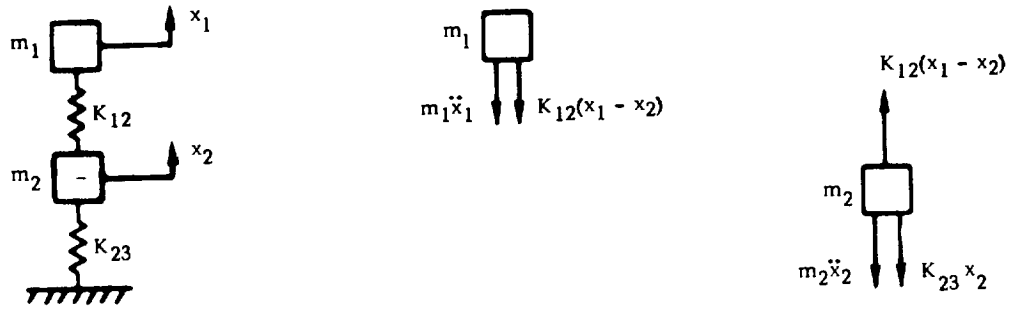

Figure 1. Two-Degree-of-Freedom System

From a consideration of equilibrium of inertial forces and spring forces under free vibration,

$$-(x_1 - x_2)\,K_{12} - m_1\,\ddot{x}_1 = 0 \tag{1}$$

$$(x_1 - x_2)\,K_{12} - K_{23}\,x_2 - m_2\,\ddot{x}_2 = 0 \tag{2}$$

or, in matrix notation, after rearranging terms,

$$\begin{bmatrix} m_1 & 0 \\ 0 & m_2 \end{bmatrix} \begin{Bmatrix} \ddot{x}_1 \\ \ddot{x}_2 \end{Bmatrix} + \begin{bmatrix} K_{12} & -K_{12} \\ -K_{12} & K_{12} + K_{23} \end{bmatrix} \begin{Bmatrix} x_1 \\ x_2 \end{Bmatrix} = 0 \tag{3}$$

or simply,

$$[M]\{\ddot{x}\} + [K]\{x\} = 0 \tag{4}$$

where the matrix containing the mass terms is the mass matrix and the matrix containing the spring or stiffness terms is the stiffness matrix.

LaGrange's equation for determining the equation of motion is

$$\frac{\partial}{\partial t}\left[\frac{\partial(KE)}{\partial \dot{q}_n}\right] + \frac{\partial(PE)}{\partial q_n} + \frac{\partial W}{\partial q_n} = 0 \tag{5}$$

where KE is the kinetic energy, PE is the potential or strain energy, W is the work done by external forces acting on the system, t is time, and q_n is a generalized coordinate of the system. For the free vibration of the system in Figure 1,

$$q_1 = x_1 \tag{6}$$

$$q_2 = x_2 \tag{7}$$

$$KE = \frac{1}{2}\left(m_1 \dot{x}_1^{\,2} + m_2 \dot{x}_2^{\,2}\right) \tag{8}$$

$$PE = \frac{1}{2}\left(x_1 - x_2\right)^2 K_{12} + \frac{1}{2} x_2^{\,2} K_{23} \tag{9}$$

$$W = 0 \tag{10}$$

Substitution of the expressions for KE, PE, and W into Equation 5 and letting $q = x_1$ yields one equation of motion; letting $q_n = x_2$ yields the second equation of motion. These are the same equations of motion derived from the consideration of equilibrium.

With the assumption of simple harmonic motion, i.e.,

$$x = x_o \sin \omega t \tag{11}$$

where x_o is an arbitrary amplitude and ω is a natural frequency, Equation 4 becomes

$$-\omega^2 [M]\{x\} + [K]\{x\} = 0 \tag{12}$$

or

$$\frac{1}{\omega^2}\{x\} = [K]^{-1}[M]\{x\}$$

$$= [\bar{D}]\{x\} \tag{13}$$

With the matrix equation in the above form, iterative methods (see Reference 8) may be used to determine the lowest and successively higher natural modes and corresponding natural frequencies. For a particular natural frequency ω_n, a set of x displacements which satisfies Equation 13 is the natural mode, $\{\phi_n\}$, corresponding to ω_n, i.e., at $\omega = \omega_n$, $\{x\} = \{\phi_n\}$. $[\bar{D}]$ is called the dynamic matrix.

The response of a vehicle to a particular forcing function may be found by summing the responses of its natural modes. The equations of motion including external forces become

$$[M]\{\ddot{x}\} + [K]\{x\} = \{F\} \tag{14}$$

The displacements $\{x\}$ may be written as the summation of the responses in the individual modes:

$$x_i = \sum_{n=1}^{n=m} \phi_{ni}\, q_n \tag{15}$$

or, in matrix notation,

$$\{x\} = [\phi]\{q\} \tag{16}$$

where

$$[\phi] = \left[\phi_1 \vdots \phi_2 \vdots \cdots \vdots \phi_m\right], \quad \{q\} = \begin{Bmatrix} q_1 \\ q_2 \\ \vdots \\ q_m \end{Bmatrix} \tag{17}$$

Substituting Equation 16 into 14,

$$[M][\phi]\{\ddot{q}\} + [K][\phi]\{q\} = \{F\} \tag{18}$$

Premultiplying each term in Equation 18 by $[\phi]^T$ yields

$$[\phi]^T [M] [\phi] \{\ddot{q}\} + [\phi]^T [K] [\phi] \{q\} = [\phi]^T \{F\} \tag{19}$$

Because of the orthogonality of natural modes with respect to the mass and stiffness matrices, i.e.,

$$\{\phi_n\}^T [M] \{\phi_s\} = \{\phi_n\}^T [K] \{\phi_s\}$$

$$= 0 \text{ for } n \neq s \tag{20}$$

the equations of motion in terms of the natural modes yield one uncoupled equation for each mode of the form

$$\{\phi_n\}^T [M] \{\phi_n\} \ddot{q}_n + \{\phi_n\}^T [K] \{\phi_n\} q_n = \{\phi_n\}^T \{F\} \tag{21}$$

The terms $\{\phi_n\}^T [M] \{\phi_n\}$ and $\{\phi_n\}^T [K] \{\phi_n\}$ are usually referred to as the generalized mass and stiffness of the n^{th} node and expressed as

$$\mathcal{M}_n = \{\phi_n\}^T [M] \{\phi_n\} \tag{22}$$

$$\kappa_n = \{\phi_n\}^T [K] \{\phi_n\} \tag{23}$$

Noting that

$$\omega_n^2 = \frac{\kappa_n}{\mathcal{M}_n} \tag{24}$$

is the square of the natural frequency of the n^{th} mode and letting the generalized force of the n^{th} mode be defined as

$$Q_n(t) = \{\phi_n\}^T \{F\} \tag{25}$$

Equation 21 becomes

$$\ddot{q}_n + \omega_n^2 q_n = \frac{Q_n(t)}{\mathcal{M}_n} \tag{26}$$

The modal amplitude (generalized coordinate) q_n may be found for each mode as a function of time from Equation 26, and then the total response may be found from Equation 16.

Then, to determine the response of a structure using modal properties, a model that yields mass and stiffness matrices for determining modal properties is desired. The selection of the specific model must be made in a manner such that modal properties are accurately defined where forces are applied and such that resulting modes give accurate values of the generalized mass. The model must be defined in enough detail to provide accurate response information in the area of interest on the vehicle.

3.1 LIQUID-PROPELLANT VEHICLE

A vehicle may be made up of several stages, with the major components by weight being propellant tanks, engines, payload, and fairings. Propellant tanks represent important portions of the liquid-propellant vehicle model since propellant weight is a large part of vehicle weight throughout most of the flight. Tank models are particularly important at liftoff when the tanks are full and for vehicles with only a few stages.

Tank models may be of the lumped parameter (spring-mass) type, which are often adequate to represent the dynamic characteristics of certain types of tanks, particularly cylinders. Continuous representations of the tanks may also be used. The method of Reference 5 uses sets of assumed displacement functions for tank elements in a manner that takes into account tank shapes made up of cylindrical, ellipsiodal, and conical elements.

The models for structural elements not containing liquid may be represented by simply the effective longitudinal stiffnesses of the structural element. This stiffness may be determined by tests or by detailed analysis using methods for developing multidimensional stiffness matrices of structures, such as the methods discussed in Reference 6.

In the following paragraphs, spring-mass models for various forms of cylindrical tanks and models based on References 2 and 3 are discussed.

3.1.1 SELECTION OF MASSES.

The number of degrees of freedom of a model determines the theoretical number of modes and frequencies. However, for a model with a large number of degrees of freedom, only a limited number of modes and frequencies may be determined accurately, and only the characteristics of the lowest modes are generally of interest. As mentioned above, the major portion of vehicle weight is propellant weight throughout much of the vehicle flight. The model of each propellant tank must represent the significant longitudinal modes of the tank in the frequency range of interest for the vehicle. This frequency range is generally from 5 to 30 Hz for liquid-propellant launch vehicles. When lower stage liquid tanks are full, several longitudinal degrees of freedom of the propellant mass might need to be included in a model to represent the lowest four or five elastic modes of the vehicle. As propellant tanks become more nearly empty, a single-longitudinal-degree-of-freedom representation of a propellant mass may be all that is required to compute the lowest four or five vehicle modes.

The details of the representation of other portions of the vehicle are not usually as critical as the propellant representation. Uncoupled longitudinal frequencies of engines, payloads, and fairings may be well above the lower vehicle frequencies, and therefore these components might be represented by a single lumped mass, or in more detail if desired. In a vehicle with a large number of stages the interstage stiffnesses may be relatively flexible and have a more dominant effect than upper stage tank stiffnesses on the vehicle lower modes and frequencies. In such instances upper stages might be represented by lumped masses connected by the interstage stiffnesses. In other words portions of the vehicle which are relatively rigid (have high uncoupled natural frequencies) might be considered as lumped masses, whereas portions of the vehicle which have low uncoupled natural frequencies and large masses must be modeled in enough detail to represent these frequencies.

3.1.2 LIQUID PROPELLANT AND TANK REPRESENTATION: SPRING-MASS MODELS. In the discussion below, simple single-degree-of-freedom spring-mass model representations are developed for cylindrical tanks. The flexibility of an elliptical tank bottom is included based on the results of Reference 4. Effects of stringers and buckled skin are considered as variations of the basic model. A model for small ullage is developed for use in analysis of tank pressure regulation systems. Models for several degrees of freedom and for cone-cylinder tanks are also considered. These models are based on models developed in References 2 and 3.

The analysis of a coupled elastic tank and propellant mass, even for a highly simplified case, becomes a very complicated eigenvalue problem. Specifically, a solution must be obtained that satisfies the differential equations for the liquid and the elastic shell, as well as appropriate boundary conditions at the tank walls, the tank bottom, and the liquid free surface. A rigorous analysis of this type is reported in Reference 1. The results yield the natural frequencies for the tank and propellant.

A number of other analyses have also been attempted for the coupled liquid and elastic container. Most of these generate a great deal of mathematical analysis that is of very little use in defining an analytical model for the tank. It is apparent, then, that other, more simplified techniques must be used. The continuous analysis can then be used as a check on the dynamic characteristics of the simplified representation.

A major building block in the development of a longitudinal structural model is a lumped parameter model for each propellant tank. In general, such tank models have been restricted to a single (predominant) mode of the coupled elastic shell and propellant mass. However, there is reason to believe that a single-mode model is not adequate in all cases. Furthermore, the development of a multimode model for the propellant tank is feasible.

As a basis for developing a tank model, first it is necessary to establish a set of approximate equations for the shell and the liquid. For example, consider the tank

shown in Figure 2, filled to a height L with a nonviscous, incompressible liquid, where the axial acceleration of the fluid is $\ddot{x}$. If it is assumed that the tank shell is thin, that any effects of preloading can be neglected, and that the loading is axially symmetric, then the following equations can be developed (Reference 10).

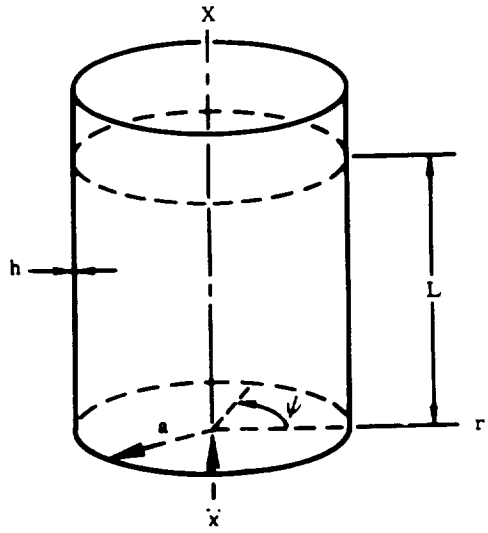

Figure 2. Cylindrical Tank and Liquid

$$\frac{Eh^3}{12\,(1-\nu^2)}\,\frac{d^4 w_r}{dX^4} + \frac{Eh}{a^2}\,W_r + \frac{\nu}{a}\,N_X = p\Big]_{r=a} \qquad (27)$$

$$\frac{du_X}{dX} = \frac{1-\nu^2}{Eh}\,N_X - \frac{\nu}{a}\,w_r \qquad (28)$$

where

w_r = the radial displacement of a shell element

u_X = the longitudinal displacement of a shell element

N_X = the axial force/unit circumferential length

p = the liquid pressure

E = Young's modulus

ν = Poisson's ratio

a = the shell radius

h = the shell thickness

Equations 27 and 28 are essentially the same as those defined for a cylindrical shell (Reference 9) and a static loading condition. If, in addition, the shell is very thin, the $\frac{d^4 w_r}{dX^4}$ term contributes very little to the gross deformation of the shell. Neglecting this term, Equation 27 becomes

$$w_r = \frac{a^2}{Eh} p \Big]_{r=a} - \frac{a\nu}{Eh} N_X \tag{29}$$

For a nonviscous, incompressible liquid, the fluid velocities are defined in terms of a velocity potential Φ by Laplace's equation, i.e.,

$$\frac{\partial^2 \Phi}{\partial r^2} + \frac{1}{r}\frac{\partial \Phi}{\partial r} + \frac{1}{r^2}\frac{\partial^2 \Phi}{\partial \psi^2} + \frac{\partial^2 \Phi}{\partial X^2} = 0 \tag{30}$$

where

$$-\frac{\partial \Phi}{\partial r} = \frac{dr}{dt}$$

$$-\frac{1}{r}\frac{\partial \Phi}{\partial \psi} = r\frac{d\psi}{dt}$$

$$-\frac{\partial \Phi}{\partial X} = \frac{dx}{dt}$$

When all forces applied to the fluid are axially symmetric, Φ is not a function of the coordinate ψ and Equation 30 reduces to

$$\frac{\partial^2 \Phi}{\partial r^2} + \frac{1}{r}\frac{\partial \Phi}{\partial r} + \frac{\partial^2 \Phi}{\partial X^2} = 0 \tag{31}$$

For small fluid velocities, the total fluid pressure is given by

$$p = \rho\left[\frac{\partial \Phi}{\partial t} + \ddot{x}(X - L)\right] \tag{32}$$

Equations 28, 29, 31, and 32 are used along with the appropriate boundary conditions of the liquid surface, tank wall, and tank bottom to form the basis for the analysis given in Reference 10. In this analysis, the effects of shell inertia for a thin shell are neglected in comparison to the liquid inertia, such that Equations 28 and 29 also apply to the dynamic condition.

In order to further simplify the development of a lumped parameter model, the velocity potential term in Equation 32 is usually neglected; i.e., the following approximation is made:

$$p \cong \rho\,\ddot{x}\,(L - X) \tag{33}$$

Equations 28, 29, and 33 are then used to develop the tank model. This neglects all contributions due to the liquid velocities, as defined by the velocity potential Φ, and the liquid-free surface waves.

Equations 28, 29, and 33 can also be used as a basis for developing a multimode tank model by dividing the tank into two or more sections. This approach can account for the higher tank modes as well as variations in tank geometry and skin thickness.

The propellant tank most commonly encountered is usually an internally pressurized circular cylinder with a rounded bottom. In many cases, the bottom is approximately elliptical in shape and can be either concave upward or downward.

In this section, a basic single-mode tank model is developed for the case of a large tank ullage volume where the pressure essentially remains constant. This model is then modified to account for the individual effects of stringer reinforcement and a buckled skin with stringer reinforcement.

3.1.2.1 Basic Single-Mass Model. The tank shown in Figure 3 is partially filled with an incompressible liquid to a depth L and the tank ullage is pressurized with a gas to some constant pressure. The tank is an elastic circular cylinder with a radius a and a constant thickness h. The tank bottom, also elastic, has an elliptical shape, where the major semi-axis is a and the minor semi-axis is b. The bottom can be either concave upward or downward. In addition, it is assumed that all loading on the tank and liquid is axisymmetric.

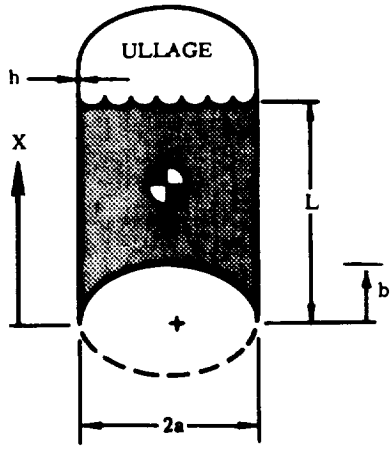

Figure 3. Partially Filled Tank

For an axial acceleration of $\ddot{x}$, the liquid pressure acting upon the wetted portion of the tank is given by Equation 33. Hoop stresses are produced in the tank skin due to this pressure. These stresses result in radial and longitudinal displacements for each element of the tank with respect to the bottom. The radial displacement, which is proportional to the pressure, is shown in Figure 4a.

When the tank is assembled with a vehicle, an acceleration of the masses above the tank results in a longitudinal force acting on the top of the tank. This force produces an additional axial stress in the tank skin and displaces the tank and the liquid center of gravity.

A flexibility matrix can be developed relating displacements at $X = L$ and center of gravity of the tank to a force at $X = L$ and an effective "liquid inertial force" acting at the center of gravity of the liquid when the bottom of the tank is fixed as shown in Figure 4. A stiffness matrix and a corresponding model for the tank can then be

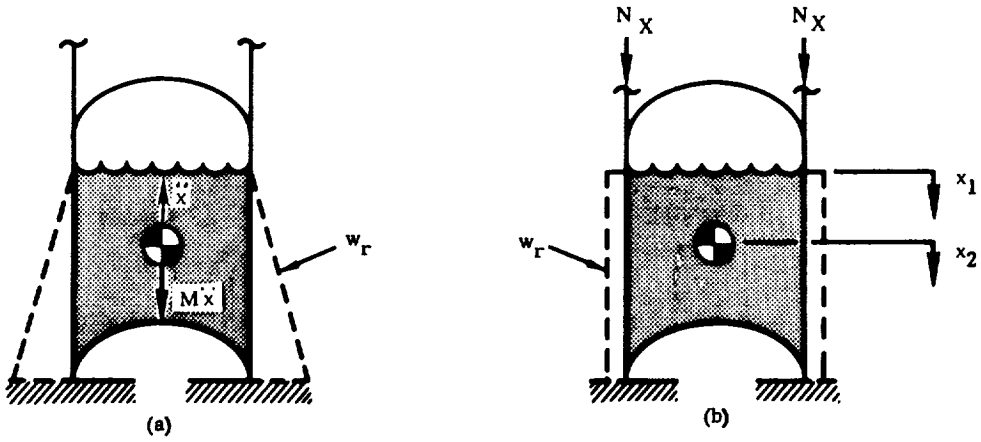

Figure 4. Tank Strains

developed. This approach yields a single-mass tank model similar to that obtained in References 10 and 2.

The equivalent single-mass model is indicated in Figure 5. Nodes 1 and 2 of the lumped parameter model are used to signify, respectively, the tank at X = L and the liquid center of gravity. The displacements of these points relative to the tank bottom (i.e., relative to X = 0 in Figure 3) are denoted by x_1 and x_2. The force acting at the top of the tank is F_1 and the effective force acting at the center of gravity is F_2, the total inertial force of the fluid due to $\ddot{x}$, i.e.,

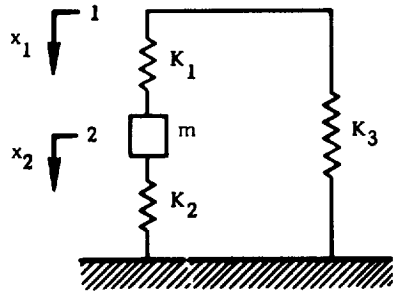

Figure 5. Equivalent Tank Model

$$F_2 = V \rho \ddot{x} = m \ddot{x} \tag{34}$$

where V, ρ, $\ddot{x}$, and m are the tank volume, fluid mass density, fluid acceleration, and the fluid mass, respectively. The liquid volume V for the cylindrical tank with an elliptical bottom is given by

$$V = \pi a^2 L D \tag{35}$$

where

$$D = 1 - \frac{2}{3}\frac{b}{L} \tag{36}$$

Therefore

$$F_2 = \pi a^2 L D \rho \ddot{x} \tag{37}$$

$$\rho \ddot{x} = \frac{F_2}{\pi a^2 LD} \tag{38}$$

It should be noted that when the bulkhead in Figure 3 is inverted (the dashed line), b takes on a negative value but the above expressions remain valid.

The relationship between displacements and the liquid inertial force are developed first. The longitudinal and circumferential stresses and strains in the thin tank skin due to the fluid pressure, p, are (to a close approximation) given by

$$\left.\begin{aligned} \sigma_x &= 0 \\ \sigma_y &= \frac{pa}{h} \\ \epsilon_x &= \frac{\nu pa}{Eh} \\ \epsilon_y &= \frac{pa}{Eh} \end{aligned}\right\} \tag{39}$$

where σ_x and σ_y are the tank longitudinal and hoop stresses, ϵ_x and ϵ_y are the longitudinal and hoop strains, ν is Poisson's ratio, and E is Young's modulus. Positive stresses are defined to be compressive in the longitudinal direction and tensile in the hoop direction; positive displacements of the tank top and liquid center of gravity are downward.

The longitudinal displacement of the tank at the liquid surface due to the fluid pressure, p, is

$$x_{12} = \int_0^L \epsilon_x \, dX \tag{40}$$

where ϵ_x is given by Equation 39. Thus, substituting Equation 33 into 39,

$$x_{12} = \int_0^L \frac{\nu a \rho \ddot{x} (L - X) \, dX}{Eh} = \frac{\nu a L^2 \rho \ddot{x}}{2Eh} \tag{41}$$

Substituting in the expression for $\rho \ddot{x}$ from Equation 38 yields

$$x_{12} = \frac{\nu L F_2}{2\pi DEha} \tag{42}$$

The tank wall radial displacement, w_r, due to p (Equation 33) is given by

$$w_r = a\epsilon_y = \frac{pa^2}{Eh} = \frac{\rho a^2 (L - X)\ddot{x}}{Eh} \tag{43}$$

The displacement of the center of gravity due to w_r and the tank bottom stiffness is then approximated by

$$x_{22} = \frac{2L}{3V}\int_0^L 2\pi a w_r\, dX + \frac{F_2}{K_B} = \frac{2}{3}\frac{\rho\ddot{x}aL^2}{DEh} + \frac{F_2}{K_B} \tag{44}$$

where K_B is the tank lower bulkhead stiffness (the appropriate values for K_B are defined parametrically later). Substituting Equation 38 for $\rho\ddot{x}$ into Equation 34 yields

$$x_{22} = \frac{2LF_2}{3\pi a D^2 Eh} + \frac{F_2}{K_B}. \tag{45}$$

Considering an axial load acting on the tank, as shown in Figure 4b, F_1 is an axial load in the tank skin resulting in a load per unit circumferential length of the tank skin given by

$$N_x = \frac{F_1}{2\pi a} \tag{46}$$

The stresses and strains in the tank due to F_1 are

$$\left.\begin{aligned} \sigma_x &= \frac{F_1}{2\pi ah} \\ \sigma_y &= 0 \\ \epsilon_x &= \frac{F_1}{2\pi aEh} \\ \epsilon_y &= \frac{\nu F_1}{2\pi aEh} \end{aligned}\right\} \tag{47}$$

while the displacements of the tank at X = L and center of gravity due to F_1 are

$$x_{11} = \int_0^L \epsilon_x\, dX = \frac{LF_1}{2\pi aEh} \tag{48}$$

$$x_{21} = \frac{L}{2} \int_0^L 2\pi a^2 \epsilon_y \, dX \cdot \frac{1}{V} = \frac{\nu L F_1}{2\pi a D E h} \tag{49}$$

The axial stiffness of the tank skin is

$$K = \frac{2\pi a E h}{L} \tag{50}$$

Then the relationships between forces and displacements from Equations 42, 45, 48, and 49 are

$$\left.\begin{aligned} d_{11} &= \frac{x_{11}}{F_1} = \frac{1}{K} \\ d_{12} &= \frac{x_{12}}{F_2} = \frac{\nu}{DK} \\ d_{21} &= \frac{x_{21}}{F_1} = \frac{\nu}{DK} \\ d_{22} &= \frac{x_{22}}{F_2} = \frac{4}{3D^2K} + \frac{1}{K_B} \end{aligned}\right\} \tag{51}$$

or, in matrix notation,

$$\begin{Bmatrix} x_1 \\ x_2 \end{Bmatrix} = \begin{bmatrix} d_{11} & d_{12} \\ d_{21} & d_{22} \end{bmatrix} \begin{Bmatrix} F_1 \\ F_2 \end{Bmatrix} = [d]\,|F| \tag{52}$$

The [d] matrix in Equation 51 can be inverted to obtain a stiffness matrix for the tank. The springs of the equivalent model for the tank can be obtained from this matrix. From Equation 51, F_1 and F_2 are

$$F_1 = \frac{4K + \frac{3D^2K^2}{K_B}}{4 - 3\nu^2 + \frac{3D^2K}{K_B}} x_1 - \frac{3\nu DK}{4 - 3\nu^2 + \frac{3D^2K}{K_B}} x_2 \tag{53}$$

$$F_2 = \frac{-3\nu\ DK}{4 - 3\nu^2 + 3D^2\frac{K}{K_B}} x_1 + \frac{3D^2K}{4 - 3\nu^2 + 3D^2\frac{K}{K_B}} x_2 \tag{54}$$

or, in matrix notation,

$$\begin{Bmatrix} F_1 \\ F_2 \end{Bmatrix} = \begin{bmatrix} K_{11} & K_{12} \\ K_{21} & K_{22} \end{bmatrix} \begin{Bmatrix} x_1 \\ x_2 \end{Bmatrix} \tag{55}$$

Therefore,

$$\left.\begin{aligned} K_{11} &= \frac{4K + 3D^2\frac{K^2}{K_B}}{4 - 3\nu^2 + 3D^2\frac{K}{K_B}} \\ K_{12} = K_{21} &= \frac{-3\nu DK}{4 - 3\nu^2 + 3D^2\frac{K}{K_B}} \\ K_{22} &= \frac{3D^2K}{4 - 3\nu^2 + 3D^2\frac{K}{K_B}} \end{aligned}\right\} \tag{56}$$

The springs of the equivalent tank model shown in Figure 5, determined from the coefficients of the stiffness matrix (as indicated in Reference 6), are

$$\left.\begin{aligned} K_1 &= -K_{12} \\ K_2 &= K_{22} + K_{12} \\ K_3 &= K_{11} + K_{12} \end{aligned}\right\} \tag{57}$$

Thus,

$$K_1 = \frac{3\nu DK}{4 - 3\nu^2 + 3D^2\frac{K}{K_B}} \tag{58}$$

$$K_2 = \frac{3D(D-\nu)K}{4 - 3\nu^2 + 3D^2\frac{K}{K_B}} \qquad (58)$$
(Contd)

$$K_3 = \frac{\left(4 - 3\nu D + 3D^2\frac{K}{K_B}\right)K}{4 - 3\nu^2 + 3D^2\frac{K}{K_B}} \qquad (59)$$

3.1.2.2 Spring Rate for Elliptical Tank Bottom. In Reference 4, spring constants are presented for ellipsoidal tank bottoms, as determined from an analysis using linear membrane theory. Graphs from which the spring constants can be obtained are reproduced here.

Consider, once again, the tank shown in Figure 3. From Reference 4 the tank bottom spring rate is given by:

$$K_B = E h_B \frac{2\pi(3e - 2f)^2}{9\left[H(f, \nu) - 2eG(f, \nu) + e^2 F(f, \nu)\right]} \qquad (60)$$

where

E = Young's modulus

h_B = bulkhead thickness

a = radius of cylinder

b = bulkhead semiminor axis

L = height of liquid in cylindrical portion of tank

e = L/a

f = b/a

ν = Poisson's ratio

The functions $H(f,\nu)$, $G(,\nu)$, and $F(f,\nu)$ are given in Figures 6, 7, and 8. These functions are derived in Reference 4.

When the tank bottom is inverted as indicated by the dashed lines in Figure 3 the expression for the spring rate becomes

$$K'_B = E h_B \frac{2\pi (3e + 2f)^2}{9\left[H(f, \nu) + 2eG(f, \nu) + e^2 F(f, \nu)\right]} \quad (61)$$

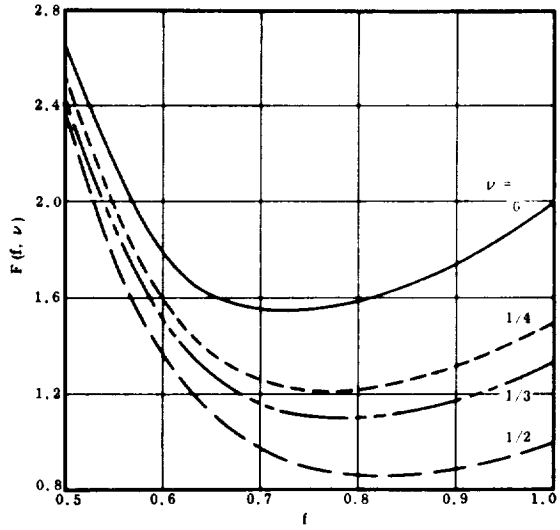

Figure 6. Variation of F(f,ν) with Depth-to-Radius Ratio for Various Values of Poisson's Ratio

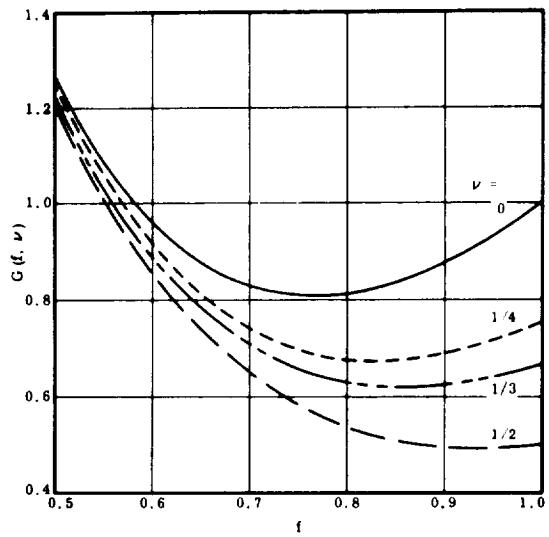

Figure 7. Variation of G(f,ν) with Depth-to-Radius Ratio for Various Values of Poisson's Ratio

3.1.2.3 Tank with Stringers and Buckled Skin. A model cylinder with skin and stringer construction is shown in Figure 9. If the stringers have negligible radial stiffness and the skin is unbuckled and can displace longitudinally and radially, the tank models described in the preceding subsections can be combined in parallel with a spring K_s, where

$$K_s = \frac{(AE)}{L} \text{ stringers} \quad (62)$$

is the total axial stiffness of the stringers in the cross-section.

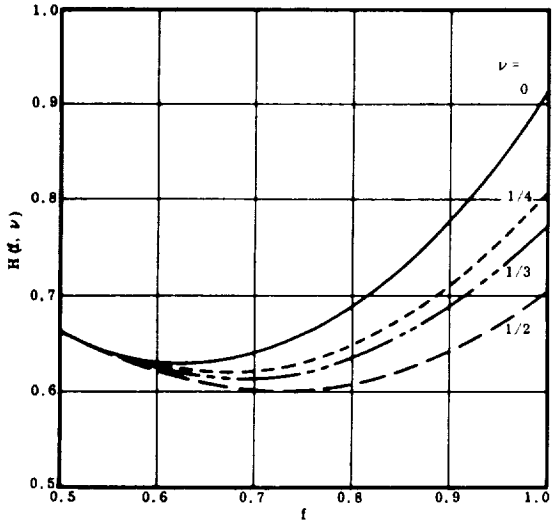

Figure 8. Variation of H(f,ν) with Depth-to-Radius Ratio for Various Values of Poisson's Ratio

When the skin is partially buckled in the axial direction, the axial stiffness of the tank skin is

$$K_{Bu} = \left[\frac{(AE) \text{ skin}}{L}\right] \text{ effective} \quad (63)$$

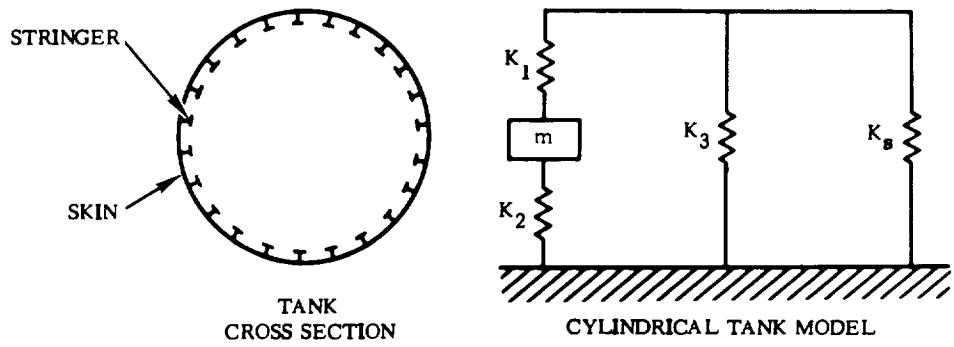

Figure 9. Skin-Stringer Cylinder Tank Model

and the flexibility coefficient d_{11} in Equation 51 becomes

$$d_{11} = \frac{1}{K_{Bu} + K_s} \tag{64}$$

The center-of-gravity displacement due to the axial load F_{Bu} carried by the buckled skin is then (neglecting the bulkhead and liquid compressibility effects)

$$x_{21} = \frac{\nu F_{Bu}}{K} \tag{65}$$

where K is the axial spring constant for the skin when unbuckled, Equation 50. That portion of the load carried by the buckled skin is given by

$$F_{Bu} = \frac{K_{Bu} F_1}{K_{Bu} + K_s} \tag{66}$$

where F_1 is the total axial load carried by the skin and stringers. Then

$$x_{21} = \frac{\nu K_{Bu} F_1}{K (K_{Bu} + K_s)} \tag{67}$$

and

$$d_{21} = \frac{x_{21}}{F_1} = \frac{\nu K_{Bu}}{K (K_{Bu} + K_s)} \tag{68}$$

The center-of-gravity displacement due to acceleration of the liquid in the tank is still (neglecting bulkhead and compressibility effects)

$$d_{22} = \frac{4}{3K} \tag{69}$$

Consequently, the flexibility matrix becomes

$$[d] = \begin{bmatrix} \dfrac{1}{K_{Bu} + K_s} & \dfrac{\nu K_{Bu}}{K(K_{Bu} + K_s)} \\ \dfrac{\nu K_{Bu}}{K(K_{Bu} + K_s)} & \dfrac{4}{3K} \end{bmatrix} \tag{70}$$

After inverting the [d] matrix and solving for the spring rates, the values for the model in Figure 10 are

$$\left.\begin{aligned} K_1 &= \frac{3\nu K_{Bu}}{4 - \dfrac{3\nu^2 K_{Bu}^2}{K(K_{Bu} + K_s)}} \\ K_2 &= \frac{3K - 3\nu K_{Bu}}{4 - \dfrac{3\nu^2 K_{Bu}^2}{K(K_{Bu} + K_s)}} \\ K_3 &= \frac{(4 - 3\nu) K_{Bu} + 4K_s}{4 - \dfrac{3\nu^2 K_{Bu}^2}{K(K_{Bu} + K_s)}} \end{aligned}\right\} \tag{71}$$

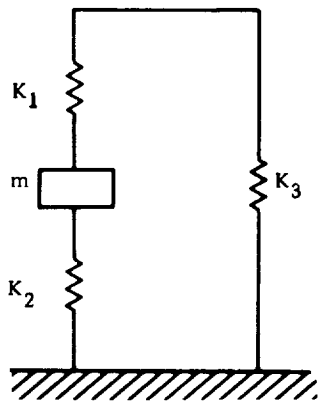

Figure 10. Skin-Stringer Model with Buckled Skin

3.1.2.4 Effects of Small Ullage Volumes. When the tank ullage volume is small, any longitudinal oscillation of the structure can produce a corresponding oscillation of significant magnitude in the ullage pressure. This can be the result of a longitudinal force transient such as thrust buildup or launcher release.

The change in ullage pressure is due to a change in ullage volume and ullage gas weight (if a pressure regulator is involved). In this section, a single-mode tank model is developed for such a case. The effect of gas compressibility is included in the model spring rates while the pressure change associated with a change in gas weight is used as the forcing function for the tank.

In order to formulate an analytical representation for the perturbation changes in the tank ullage, the following assumptions are made.

a. The gas, or mixture of gases, in the tank ullage behaves in a quasi-static manner.

b. The gas process is adiabatic.

c. The perturbation variables are small.

The equation of state for a gas (or a mixture of gases) at low pressure is given to a close approximation by the equation below:

$$PV = WR_m T \tag{72}$$

where P is pressure, V is volume, W is weight, T is temperature, and R_m is the gas constant for the mixture. In a strict sense, Equation 72 applies to a condition of thermodynamic equilibrium. It also applies (approximately) for a perturbation condition when the changes in these variables are slow enough, and small enough, such that the gas is at all times close to thermodynamic equilibrium. The gas is then said to behave in a quasi-static manner.

For an additional relationship between the variables in the tank ullage, it is convenient to assume that the process is adiabatic. In such case,

$$T \propto P^{\left(\frac{\gamma_m - 1}{\gamma_m}\right)} \tag{73}$$

where γ_m is the adiabatic exponent for the gas. In general, a polytropic exponent would be used for Equation 73. However, in the frequency range of interest it can be assumed that there is little chance for heat transfer to the gas so that the polytropic exponent is close to the adiabatic value.

Equations 72 and 73 can now be combined to form the following equation:

$$P = \text{const.}\left(\frac{WR_m}{V}\right)^{\gamma_m} \tag{74}$$

A given tank may contain a mixture of gases. The total weight is then given by

$$W = W_1 + W_2 + \ldots \tag{75}$$

and the effective gas constant, R_m, is defined by

$$R_m = \frac{W_1 R_1 + W_2 R_2 + \ldots}{W} \tag{76}$$

where R_1, R_2, etc., are the gas constants for the individual gases.

For small perturbations during flight, the change in tank pressure is defined by the first terms of a Taylor's series, where the partial derivatives are evaluated at the steady-state (or equilibrium) condition, i.e.,

$$\Delta P = \left.\frac{\partial P}{\partial W}\right]_{s.s.} \Delta W + \left.\frac{\partial P}{\partial V}\right]_{s.s.} \Delta V \tag{77}$$

where ΔW is the change in ullage gas weight and ΔV the change in ullage volume.

For the steady-state condition,

$$\bar{P} = \text{const.}\left(\frac{\bar{W} R_m}{\bar{V}}\right)^{\gamma_m} \tag{78}$$

The partial derivatives in Equation 77 can be evaluated by using Equation 78 to define the proportionality constant, so that

$$\Delta P = p_a = K_w \frac{\dot{w}}{s} - K_v v \tag{79}$$

where s is the Laplace operator, and

$$\left.\begin{aligned} K_w &= \frac{\gamma_m \bar{P} R_g}{\bar{W} R_m} \\ K_v &= \frac{\gamma_m \bar{P}}{\bar{V}} \end{aligned}\right\} \tag{80}$$

where R_g is the gas constant for the pressurizing gas and where $\dot{w} = \Delta\dot{W}$, $v = \Delta V$, and the bars denote steady-state quantities.

Figure 11 shows a thin skin, cylindrical tank shell with an elliptical bulkhead for the bottom. The top of the tank is assumed to be rigid and the tank is nearly filled with liquid. Forces F_1 acting on the top of the tank, an effective inertial force, F_2, acting at the liquid center of gravity, and an ullage pressure change, p_a', acting in the ullage space are also shown. The pressure change p_a' represents only that portion of the total pressure change in the ullage that can be attributed to a change in gas weight. The compressibility effect, due to a change in ullage volume, is included in the model spring rates. Therefore, from Equation 79, p_a' is defined by

$$s p_a' = K_w \dot{w} \tag{81}$$

or

$$p_a' = p_a + K_v v \tag{82}$$

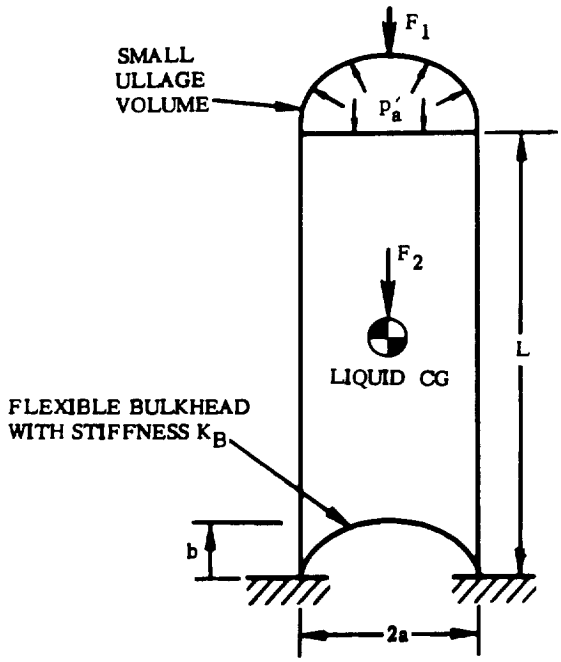

Figure 11. Tank with Small Ullage Volume

If the displacements of the tank top and liquid center of gravity are x_1 and x_2, and the change in ullage volume is v_a, then the relationship between forces, pressure, displacement, and change in ullage volume is given by the matrix equations

$$\begin{vmatrix} x_1 \\ x_2 \\ v_a \end{vmatrix} = \begin{bmatrix} \bar{d}_{11} & \bar{d}_{12} & \bar{d}_{1v} \\ \bar{d}_{21} & \bar{d}_{22} & \bar{d}_{2v} \\ \bar{d}_{v1} & \bar{d}_{v2} & \bar{d}_{vv} \end{bmatrix} \begin{vmatrix} F_1 \\ F_2 \\ p'_a \end{vmatrix} = [\bar{d}] \, |F| \tag{83}$$

or

$$\left|\begin{array}{c} x_1 \\ \hline x_2 \\ \hline v_a \end{array}\right| = \left[\begin{array}{c|c|c} d_{11} - \dfrac{d_{v1}^2}{C + d_{vv}} & d_{21} - \dfrac{d_{2v}\, d_{v1}}{C + d_{vv}} & \dfrac{C\, d_{v1}}{C + d_{vv}} \\ \hline d_{12} - \dfrac{d_{1v}\, d_{v2}}{C + d_{vv}} & d_{22} - \dfrac{d_{2v}^2}{C + d_{vv}} & \dfrac{C\, d_{v2}}{C + d_{vv}} \\ \hline \dfrac{C\, d_{1v}}{C + d_{vv}} & \dfrac{C\, d_{2v}}{C + d_{vv}} & \dfrac{C\, d_{vv}}{C + d_{vv}} \end{array}\right] \left|\begin{array}{c} F_1 \\ \hline F_2 \\ \hline p'_a \end{array}\right| \tag{84}$$

where $C = \dfrac{1}{K_v}$ is the compliance of the gas in the ullage volume, and

$$\begin{bmatrix} d_{11} & d_{12} & d_{1v} \\ d_{21} & d_{22} & d_{2v} \\ d_{v1} & d_{v2} & d_{vv} \end{bmatrix} = [d]$$

$$
= \left|\begin{array}{c|c|c}
\dfrac{1}{K} & \dfrac{\nu}{DK} & \dfrac{2\pi a^2\left(\nu-\frac{1}{2}\right)}{K} \\
\hline
 & & \dfrac{2\pi a^2\left(1-\frac{\nu}{2}\right)}{DK} \\
\dfrac{\nu}{DK} & \dfrac{4}{3D^2K}+\dfrac{1}{K_B} & +\dfrac{\pi a^2}{K_B} \\
\hline
 & \dfrac{2\pi a^2\left(1-\frac{\nu}{2}\right)}{DK} & \dfrac{2\pi^2 a^4\left(\frac{5}{2}-2\nu\right)}{K} \\
\dfrac{2\pi a^2\left(\nu-\frac{1}{2}\right)}{K} & & \\
 & +\dfrac{\pi a^2}{K_B} & +\dfrac{\pi^2 a^4}{K_B}
\end{array}\right| \qquad (85)
$$

The compliance, C, could be defined to include flexibility of the tank upper bulkhead. As the ullage volume increases, C becomes infinite and the model reduces to the basic tank model.

The $[\bar{d}]$ matrix can be inverted to obtain a stiffness matrix:

$$
[\bar{d}]^{-1} = [K] = \begin{bmatrix} K_{11} & K_{12} & K_{1v} \\ K_{21} & K_{22} & K_{2v} \\ K_{v1} & K_{v2} & K_{vv} \end{bmatrix} \qquad (86)
$$

A tank model where the ullage gas compressibility is included in the spring rates and where the applied forces are due to p'_a is shown in Figure 12.

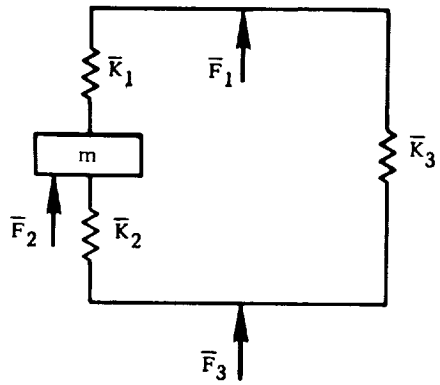

Figure 12. Tank Model for Small Ullage Volume

The tank spring rates, defined in terms of the stiffness matrix, are

$$\left.\begin{aligned} \bar{K}_1 &= -K_{12} + \frac{K_{1v}\,K_{2v}}{K_{vv}} \\ \bar{K}_2 &= K_{22} + K_{21} - \frac{K_{2v}\,K_{v1} + K_{2v}^2}{K_{vv}} \\ \bar{K}_3 &= K_{11} + K_{12} - \frac{K_{1v}\,K_{2v} + K_{1v}^2}{K_{vv}} \end{aligned}\right\} \quad (87)$$

3.1.2.5 Multimass Models. In most analyses of current vehicles, the structural representations used have been based upon the tank model shown in Figure 5. This model provides an approximation for the first (predominant) mode of the coupled propellant and elastic tank. However, it is known that higher modes exist in the tank and a limited number of these may have a significant energy content, compared to the first, and they do provide a resonant condition at discrete higher frequencies. This is shown in Reference 10.

This implies one of two conditions. Either the higher tank modes are unimportant and their omission does not affect the overall structural modes, or certain structural modes are inaccurate because of this omission. The actual condition, of course, depends upon many factors such as the type of structure, the propellant level, etc.

There has been very little opportunity to determine the accuracy of predicted vehicle modes using current models. It is believed that, in most cases, the first mode predictions are adequate and that any errors are incurred in the higher modes. This should be particularly true when the propellant mass is large and represents a major part of the vehicle mass.

It is desirable to further explore the importance or contribution of the higher tank modes by developing a multimode tank model and using it in the structural representation for the vehicle. The initial results obtained by using this approach are discussed in this subsection.

A discrete model for higher tank modes can be developed in a manner similar to that used for the single-mass representation. Consider again the cylindrical tank with an elliptical bulkhead as shown in Figure 13. Assume, for the present, that the bulkhead is inelastic (rigid) and that the liquid is incompressible.

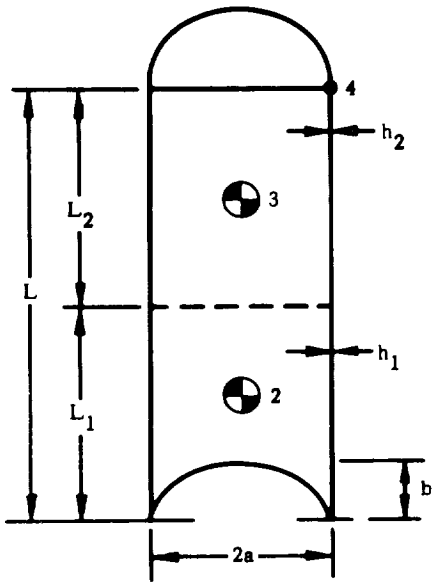

Figure 13. Two-Element Tank

Let the tank and propellant be divided into two elements. A point on the tank at the liquid surface, the center of gravity of the upper element, and the center of gravity of the lower element are denoted by Stations 4, 3, and 2, respectively. The propellant heights are L_1 and L_2 while the tank wall thicknesses are h_1 and h_2.

The procedure used to develop a two-mass model is exactly the same as that used for the single-mass model. This procedure can be expanded to any number of elements.

The following quantity is similar to that from Equation 36.

$$D_1 = 1 - \frac{2}{3}\frac{b}{L_1} \tag{88}$$

while the axial rates at the two tank elements are given by

$$\left.\begin{aligned} K_1 &= \frac{2\pi a E h_1}{L_1} \\ K_2 &= \frac{2\pi a E h_2}{L_2} \end{aligned}\right\} \tag{89}$$

Next, consider the individual effects of an axial acceleration, $\ddot{x}$, on the two fluid elements. The resulting radial deflections of the tank are shown in Figure 14a and b along with the corresponding inertial forces, F_2 and F_3, acting at the two fluid center-of-gravity locations. Finally, an external force, F_4, is considered at the top of the tank. This produces the radial tank deflection shown in Figure 14c. The individual axial and radial deflections of the shell can be evaluated using the shell equations. This leads to the following influence coefficients.

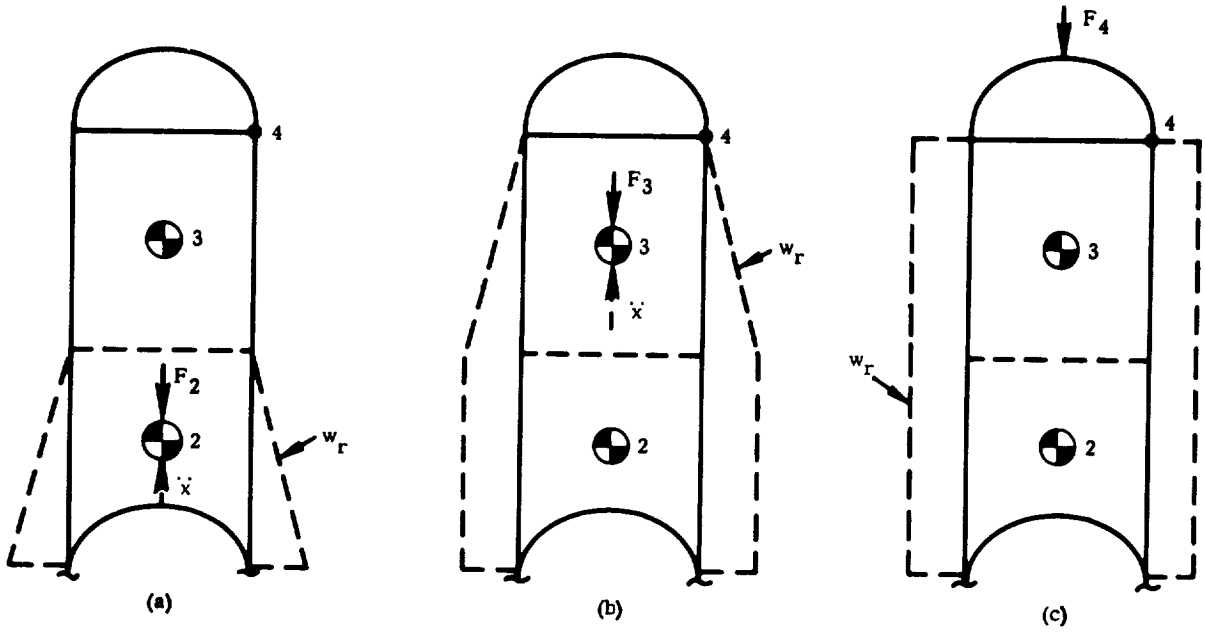

Figure 14. Assumed Forces on Two-Element Tank

$$
\left.
\begin{aligned}
d_{32} &= \frac{x_{32}}{F_2} = \frac{2}{D_1 K_1} \\
d_{22} &= \frac{x_{22}}{F_2} = \frac{4}{3 D_1^2 K_1} \\
d_{42} &= \frac{x_{42}}{F_2} = \frac{\nu}{D_1 K_1} \\
d_{23} &= \frac{x_{23}}{F_3} = \frac{2}{D_1 K_1} \\
d_{33} &= \frac{x_{33}}{F_3} = \frac{4}{K_1} + \frac{4}{3 K_2} \\
d_{43} &= \frac{x_{43}}{F_3} = \frac{2\nu}{K_1} + \frac{\nu}{K_2} \\
d_{24} &= \frac{x_{24}}{F_4} = \frac{\nu}{D_1 K_1}
\end{aligned}
\right\} \qquad (90)
$$

$$\left.\begin{aligned} d_{34} &= \frac{x_{34}}{F_4} = \frac{2\nu}{K_1} + \frac{\nu}{K_2} \\ d_{44} &= \frac{x_{44}}{F_4} = \frac{K_1 + K_2}{K_1 K_2} \end{aligned}\right\} \qquad \text{(90 Contd)}$$

The influence matrix is then given by

$$[d] = \begin{bmatrix} d_{22} & d_{23} & d_{24} \\ d_{32} & d_{33} & d_{34} \\ d_{42} & d_{43} & d_{44} \end{bmatrix} \qquad (91)$$

$$= \left[\begin{array}{c|c|c} \dfrac{4}{3D_1^2 K_1} & \dfrac{2}{D_1 K_1} & \dfrac{\nu}{D_1 K_1} \\ \hline \dfrac{2}{D_1 K_1} & \dfrac{4}{K_1} + \dfrac{4}{3K_2} & \dfrac{2\nu}{K_1} + \dfrac{\nu}{K_2} \\ \hline \dfrac{\nu}{D_1 K_1} & \dfrac{2\nu}{K_1} + \dfrac{\nu}{K_2} & \dfrac{K_1 + K_2}{K_1 K_2} \end{array}\right] \qquad (92)$$

where for $L_1 = L_2 = \frac{L}{2}$, Equations 88 and 89 become

$$\left.\begin{aligned} K_1 &= \frac{4\pi a E h_1}{L} \\ K_2 &= \frac{4\pi a E h_2}{L} \\ D_1 &= 1 - \frac{4b}{3L} \end{aligned}\right\} \qquad (93)$$

For a particular tank, the coefficients of the [d] matrix can be evaluated. The [d] matrix can then be inverted to obtain a stiffness matrix. Figure 15 shows a model which would correspond to the stiffness matrix given by

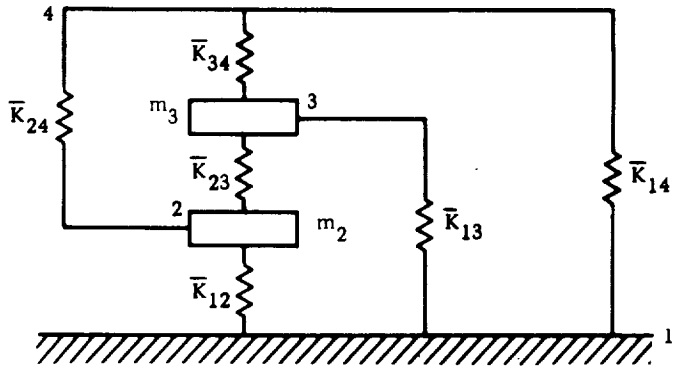

Figure 15. Two-Mass Tank Model

$$[d]^{-1} = \begin{bmatrix} K_{22} & K_{23} & K_{24} \\ K_{32} & K_{33} & K_{34} \\ K_{42} & K_{43} & K_{44} \end{bmatrix} \tag{94}$$

where the model spring stiffnesses are related to the stiffness matrix by

$$\left.\begin{aligned} \bar{K}_{23} &= -K_{23} \\ \bar{K}_{24} &= -K_{24} \\ \bar{K}_{34} &= -K_{34} \\ \bar{K}_{12} &= K_{22} + K_{23} + K_{24} \\ \bar{K}_{13} &= K_{32} + K_{33} + K_{34} \\ \bar{K}_{14} &= K_{42} + K_{43} + K_{44} \end{aligned}\right\} \tag{95}$$

This model can be generalized for many degrees of freedom by writing general expressions for the influence coefficients of a multimass model. Also, the effects of a flexible tank bottom and liquid compressibility can be included in the process.

3.1.2.6 Tanks with Conical Sections. A tank may be composed of a combination of circular cylinder and conical segments where a change in vehicle diameter is required between stages. Figure 16 shows a typical example.

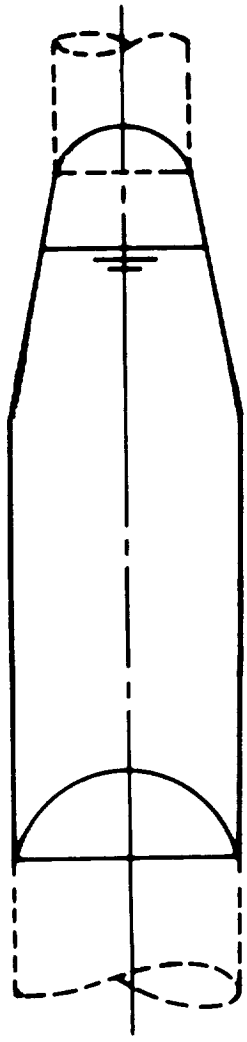

Figure 16. Vehicle with Cone-Cylinder Tank

An approximate model for a tank of this type might be determined using a cylinder having the same mass and total axial stiffness. For the tank of Figure 17, the axial stiffness is

$$K_{cc} = \int_0^L \frac{dX}{2\pi a E h}$$

$$= \frac{K_1 K_2}{K_1 + K_2} \qquad (96)$$

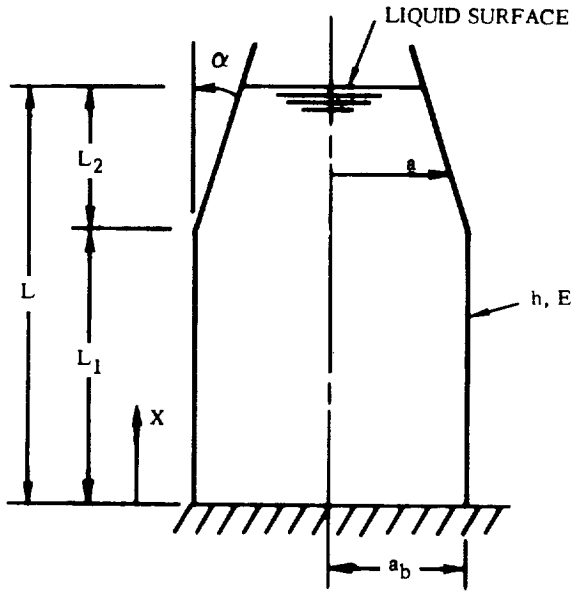

Figure 17. Cone-Cylinder Tank

where

K_1 = cylinder axial stiffness

$$= \frac{2\pi a_b E h}{L_1} \tag{97}$$

K_2 = cone axial stiffness

$$= \frac{K_1 L_1 \sin \alpha}{a_b \log\left(\frac{a_b}{a_b - L_2 \tan \alpha}\right)} \tag{98}$$

Then

$$K_{cc} = \frac{K_1}{1 + \left(\frac{a_b}{L_1 \sin \alpha}\right) \log\left(\frac{a_b}{a_b - L_2 \tan \alpha}\right)} \tag{99}$$

If m_{cc} is the total mass of the liquid in the tank, and m_{cc} and K_{cc} are used with the model of Figure 5 and Equations 56 and 57,

$$\left.\begin{aligned} K_1 &= \frac{3\nu\, K_{cc}}{4 - 3\nu^2} \\ K_2 &= \frac{3\,(1-\nu)\, K_{cc}}{4 - 3\nu^2} \\ K_3 &= \frac{(4 - 3\nu)}{4 - 3\nu^2} K_{cc} \end{aligned}\right\} \qquad (100)$$

where the model is as indicated in Figure 18.

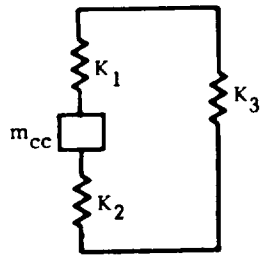

Figure 18. Equivalent Cylinder Model

This model yields only approximately the correct frequency; use of such a model in a complete vehicle indicates that its frequency is too high. For a 10-degree cone with L_1/L_2 of about 0.4 for a first-stage LO_2 tank, the resulting vehicle first-mode frequency is about 20 percent too high in the first mode when compared with flight data. As the liquid surface drops in the cone and approaches the top of the cylinder, the model frequency appears to be more accurate. The apparent error of this model seems to be related to the geometry of the cone rather than its stiffness.

An approximate model for the cone-cylinder tank could also be determined using a two-degree-of-freedom model for the tank and assuming that the cone is rigid when determining effects of propellant inertial forces. A model of this type is shown in Figure 19.

The same notation is used as in Subsection 3.1.2.5 except that now Station 3 denotes the center of gravity of the liquid in the conical section of the tank. Now consider the individual effects of an axial acceleration acting on each of the two fluid elements. The resultant radial deformations of the cylindrical portion of the tank are shown in Figure 20a and b along with the corresponding inertial forces, F_2 and F_3, acting at the two fluid center-of-gravity locations. The effect of an external force, F_4, is indicated in Figure 20c. The axial and radial deflections of the cylinder can be evaluated using equations for strain developed in a manner similar to that of Subsection 3.1.2.1. This leads to the following approximate influence coefficient matrix:

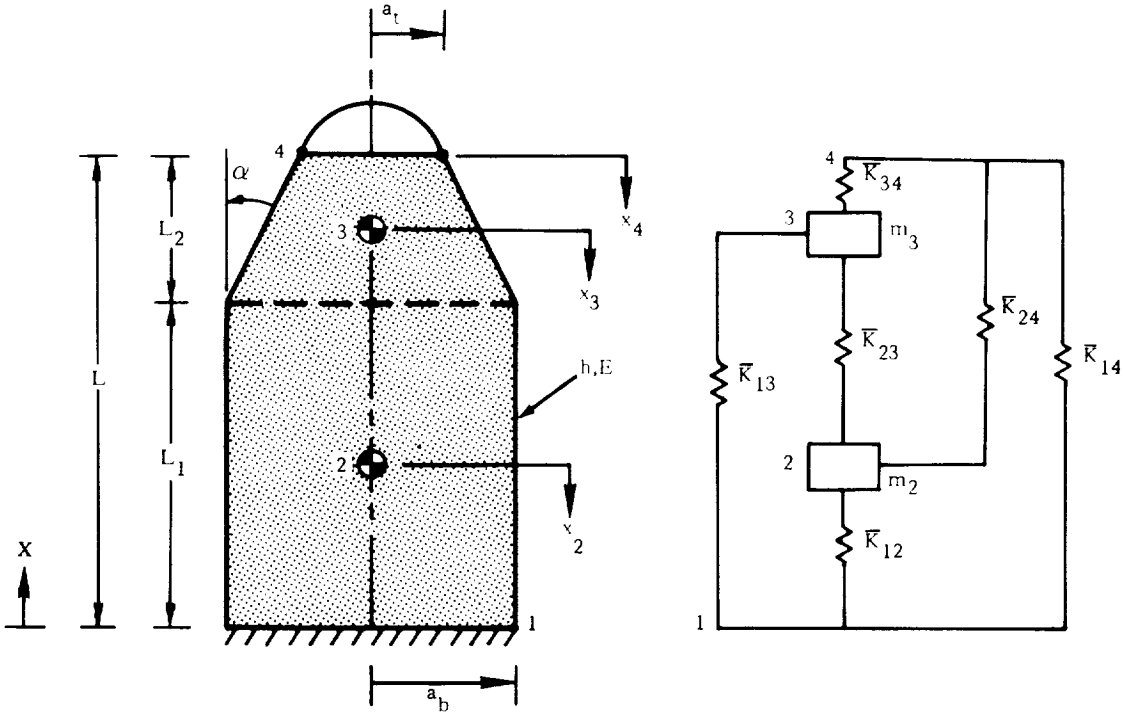

Figure 19. Two-Mass Cone-Cylinder Model

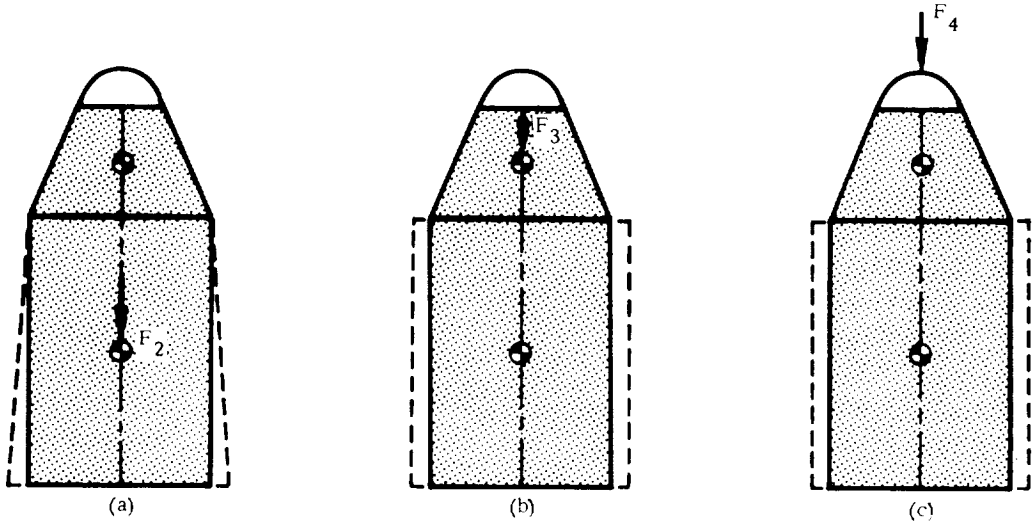

Figure 20. Radial Deformations in Two-Mass Cone-Cylinder Model

$$[d] = \begin{bmatrix} \frac{4}{3K_1} & \text{Symmetric} & \\ \frac{2C_0}{K_1} & \frac{4C_0^2}{K_1} & \\ \frac{\nu}{K_1} & \frac{2\nu C_0}{K_1} & \frac{K_1 + K_2}{K_1 K_2} \end{bmatrix} \tag{101}$$

where

$$C_0 = \frac{1}{\frac{1}{3}\left[1 + \Phi_0 + \Phi_0^2\right]} \tag{102}$$

$$\Phi_0 = \frac{a_t}{a_b} = 1 - \frac{L_2}{a_b} \tan \alpha \tag{103}$$

and

$$\begin{Bmatrix} x_2 \\ x_3 \\ x_4 \end{Bmatrix} = [d] \begin{Bmatrix} F_2 \\ F_3 \\ F_4 \end{Bmatrix} \tag{104}$$

If we want to compute the natural frequency of the tank, the displacement x_4 need not be considered:

$$-\omega^2 \begin{bmatrix} m_2 & 0 \\ 0 & m_3 \end{bmatrix} \begin{Bmatrix} x_2 \\ x_3 \end{Bmatrix} + \begin{bmatrix} d_{22} & d_{23} \\ d_{23} & d_{33} \end{bmatrix}^{-1} \begin{Bmatrix} x_2 \\ x_3 \end{Bmatrix} = 0 \tag{105}$$

A nontrivial solution of the above equation exists only if the following determinant is equal to zero:

$$\left| [d][M] - \frac{1}{\omega^2} I \right| = \begin{vmatrix} d_{22} m_2 - \frac{1}{\omega^2} & d_{23} m_3 \\ d_{23} m_2 & d_{33} m_3 - \frac{1}{\omega^2} \end{vmatrix} = 0 \tag{106}$$

where I is an identity matrix.

After substituting expressions for the influence coefficients and making the following substitutions,

$$\left.\begin{aligned} m_2 &= \pi a_b^2 L_1 \rho \\ m_3 &= \frac{\pi a_b^2 L_2 \rho}{C_0} \\ \omega_o^2 &= \frac{3K_1}{4\pi a_b^2 L_1 \rho} = \frac{3}{2}\frac{Eh}{\rho a_b L_1^2} \\ \lambda &= \left(\frac{\omega_o}{\omega}\right)^2 \\ \beta &= \frac{L_2}{L_1} \end{aligned}\right\} \quad (107)$$

then the determinant becomes

$$\begin{vmatrix} 1-\lambda & \frac{3}{2}\beta \\ \frac{3}{2}C_0 & 3\beta C_0 - \lambda \end{vmatrix} = 0 \quad (108)$$

Expansion of the determinant leads to the characteristic equation,

$$\lambda^2 - b\lambda + c = 0 \quad (109)$$

where

$$b = 1 + 3\beta C_0$$

$$c = \frac{3}{4}\beta C_0$$

Two roots for λ result from the characteristic equation. The root corresponding to the lowest natural frequency leads to

$$\left(\frac{\omega_1}{\omega_o}\right) = \left\{ \frac{2}{1 + R + \left[1 + R + R^2\right]^{1/2}} \right\}^{1/2} \tag{110}$$

where

$$R = 3\beta C_0$$

A similar equation may be derived for the "equivalent" cylinder; letting the first natural frequency from the equivalent cylinder be $\bar{\omega}_1$,

$$\left(\frac{\bar{\omega}_1}{\omega_o}\right)^2 = \left\{ \frac{1}{\left[1 + \frac{\beta}{C_0}\right]\left[1 + \frac{\gamma}{\sin\alpha} \log\left(\frac{1}{\Phi_o}\right)\right]} \right\} \tag{111}$$

where

$$\gamma = \frac{a_b}{L_1}$$

The two equations given above were evaluated for a β range of 0 to 0.5 for a tank with the following parameters:

$$\alpha = 10^\circ$$

$$a_b = 60 \text{ in.}$$

$$L_1 = 310 \text{ in.}$$

The results are shown in Figure 21. The two-degree-of-freedom model gives a frequency increasingly lower than the equivalent cylinder model as β increases, i.e., as the liquid level rises higher and higher in the cone. The value of $\beta = 0.42$ corresponds to about the propellant configuration of an Atlas LO_2 tank at liftoff. For this value of β, the natural frequency given by the equivalent cylinder model is about 17 percent higher than the value given by the cone-cylinder model.

The equivalent model for the cone-cylinder tank would be obtained by inverting the flexibility matrix of Equation 101 (in a manner similar to that of Subsection 3.1.2.5).

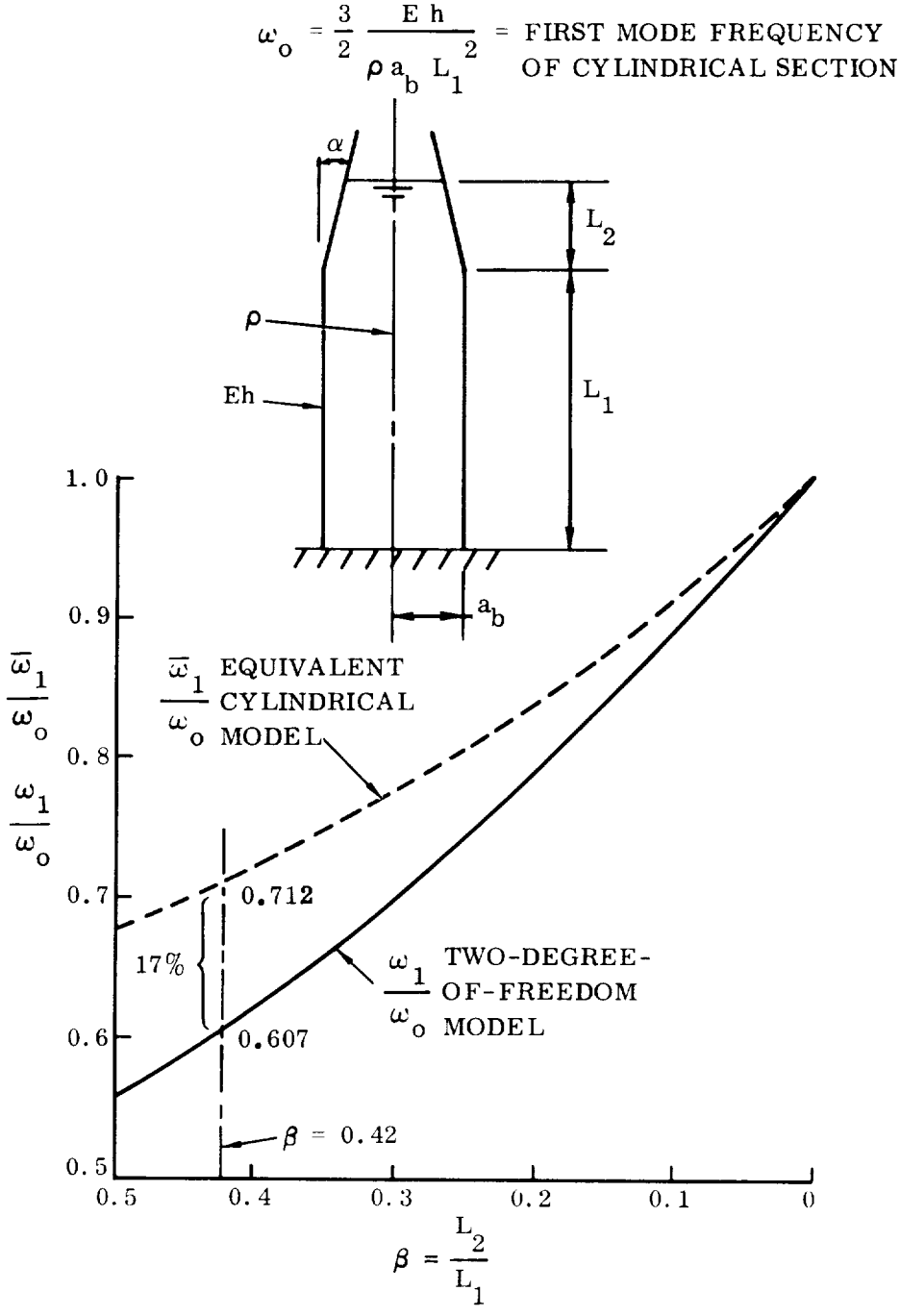

Figure 21. Natural Frequency of Cone-Cylinder Tank

$$[\bar{K}] = [d]^{-1} = \begin{bmatrix} K_{22} & K_{23} & K_{24} \\ K_{32} & K_{33} & K_{34} \\ K_{42} & K_{43} & K_{44} \end{bmatrix} \tag{112}$$

The corresponding spring-mass model (see Figure 19) is

$$\left.\begin{aligned}
\bar{K}_{23} &= -K_{23} &&= \frac{3}{2C_0} K_1 \\
\bar{K}_{24} &= -K_{24} &&= 0 \\
\bar{K}_{34} &= -K_{34} &&= \frac{\nu}{2C_0(\bar{\bar{K}} - \nu^2)} K_1 \\
\bar{K}_{12} &= K_{22} + K_{23} + K_{24} &&= \frac{(6C_0 - 3)}{2C_0} K_1 \\
\bar{K}_{13} &= K_{32} + K_{33} + K_{34} &&= \frac{4\bar{\bar{K}} - 3\nu^2 - 2C_0\nu - 6C_0(\bar{\bar{K}} - \nu^2)}{4C_0^2(\bar{\bar{K}} - \nu^2)} K_1 \\
\bar{K}_{14} &= K_{42} + K_{43} + K_{44} &&= \frac{(2C_0 - \nu)}{2C_0(\bar{\bar{K}} - \nu^2)} K_1
\end{aligned}\right\} \tag{113}$$

where

$$\bar{\bar{K}} = \frac{K_1}{K_{cc}}$$

3.1.3 LOCAL STRUCTURE EFFECTS. The stiffness of local structure may be evaluated in detail using methods for representing complex structure such as that presented in Reference 6 or by direct tests after the hardware has been built. Tests on local structure are advised where practical since difficulties are often encountered in representation of support structure for engines, payloads, and components.

3.1.4 TEMPERATURE. Extreme temperatures ranging from cryogenic to several hundred degrees Fahrenheit may affect the value of the modulus of elasticity of important portions of the vehicle structure. The correction required may affect frequencies by several percent at certain times of flight and should be taken into account if this degree of accuracy is required.

3.1.5 EFFECT OF AXIAL LOAD ON STIFFNESS OF SKIN-STRINGER STRUCTURES. This subject was covered in Subsection 3.1.2.3 in the discussion of a tank with stringers and buckled skin. Any skin and stringer structure has an axial stiffness that is the sum of the stiffnesses of the stringers plus the effective stiffness of partially buckled skin between the stringers.

3.1.6 IMPROVED ANALYTICAL MODEL. The model of Reference 5 uses a finite element technique to construct the total launch vehicle stiffness matrix [K] and mass matrix [M] by dividing the vehicle structure into axisymmetric shell, fluid, and spring-mass elements.

Axisymmetric shell elements are used to represent fairings, interstage adapters, bulkheads, and thrust structures. The fluid elements used have motions consistent with containing shell elements. Spring-mass elements are used to represent equipment and engines.

Figure 22 illustrates a vehicle and its idealization into the three basic types of elements.

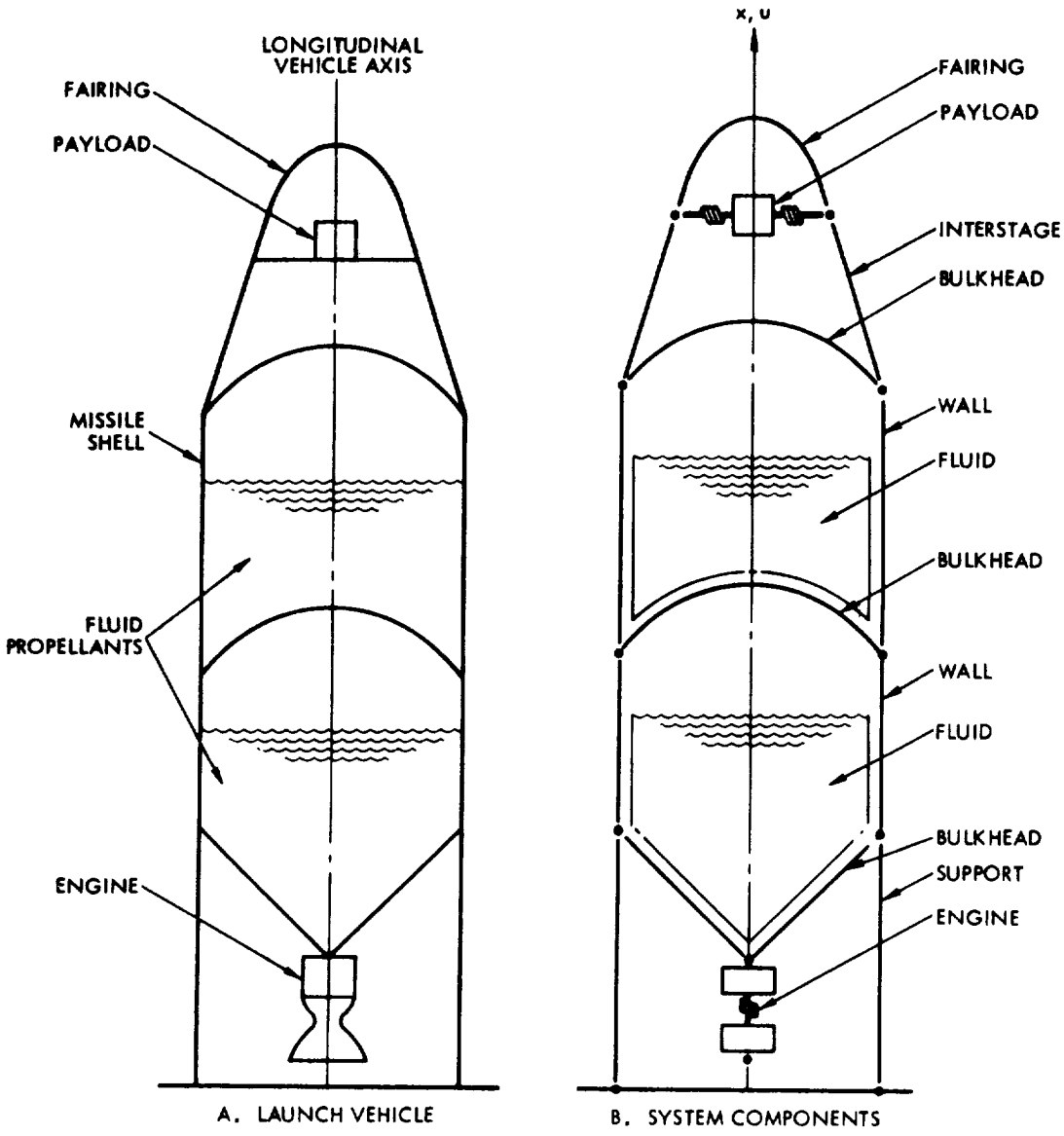

Figure 22. Vehicle and Idealization in Basic Components

†Figure reproduced from Reference 5, page 2.2.

The Rayleigh-Ritz technique is used with assumed polynomial displacement patterns to determine shell and fluid element mass and stiffness characteristics. The stiffness and mass matrices for the complete vehicle are obtained by superposition of the stiffness and mass matrices of the individual shell, fluid, and spring-mass components.

In the Rayleigh-Ritz method a stiffness matrix is determined for each element from the strain energy of the element. The strain energy of the element can be determined from the assumed displacement functions and the stress-strain laws assumed for the shell element. The strain energy for a shell of revolution due to axisymmetric loading is

$$V = \frac{1}{2}\int_s 2\pi r \left(N_\phi \epsilon_\phi + N_\theta \epsilon_\theta + M_\phi K_\phi + M_\theta K_\theta + N^\circ_\phi \rho^2\right) ds \tag{114}$$

where

$$\left.\begin{aligned}
\epsilon_\phi &= \frac{1}{r_1}\left(\frac{d\bar{V}}{d\phi} + \bar{W}\right) \\
\epsilon_\theta &= \frac{1}{r_2}\left(\bar{V}\cot\phi + \bar{W}\right) \\
K_\phi &= \frac{1}{r_1}\frac{d}{d\phi}\left[\frac{1}{r_1}\left(\frac{d\bar{W}}{d\phi} - \bar{V}\right)\right] \\
K_\theta &= \frac{\cot\phi}{r_2}\left[\frac{1}{r_1}\left(\frac{d\bar{W}}{d\phi} - \bar{V}\right)\right] \\
\rho &= \frac{1}{r_1}\frac{d\bar{W}}{d\phi} - \bar{V}
\end{aligned}\right\} \tag{115}$$

where r_1 and r_2 and the radii of curvature of the shell in the meridional and hoop directions, N°_ϕ is the initial meridional stress, and

$$\left.\begin{aligned}
N_\phi &= C_{11}\epsilon_\phi + C_{12}\epsilon_\theta \\
N_\theta &= C_{12}\epsilon_\phi + C_{22}\epsilon_\theta \\
M_\phi &= C_{33}K_\phi + C_{34}K_\theta \\
M_\theta &= C_{34}K_\phi + C_{44}K_\theta
\end{aligned}\right\} \tag{116}$$

where

$C_{11} \cdots C_{44}$ are orthotropic constants,

N_ϕ, N_θ = meridional and hoop load per unit length

M_ϕ, M_θ = meridional and hoop moment per unit length

ϵ_ϕ, ϵ_θ = meridional and hoop strain

K_ϕ, K_θ = meridional and hoop curvature

Similarly, mass properties for fluid and shell elements may be computed from their kinetic energies based on the assumed displacement functions. This method, in the current programmed form of Reference 5, has been applied to analysis of a one-tenth scale Saturn V model as reported in Reference 11.

The method appears to be the most general method available for analysis of a complete vehicle. It overcomes many of the limitations of the approximations required in developing the discrete lumped parameter models discussed earlier. In its current form (Reference 5) it will not handle such tank configurations as the cone-cylinder tank discussed in Subsection 3.1.2.6; it does not account for ullage gas effects, etc. However, the generality of the basic method would conceivably permit the model of Reference 5 to be extended to account for such effects.

3.2 ADDING COMPONENTS USING MODE SYNTHESIS

Frequently it is desirable to make a parameter study to determine the effect on vehicle response resulting from changes in the characteristics of a specific area or component, e.g., a sloshing mass or engine system. Rather than make several analyses of the system, changing but a fraction of the parameters each time, the vibration characteristics of the system excluding the specific varying parameter may be calculated, and then modified by coupling the parameter back in through the mode synthesis technique (discussed in References 12 and 13).

The equations of motion may be written for all components of a system. The equations may be written compactly in the uncoupled form for components of a system having an arbitrary number of components. Interpreted physically, this can be considered to be a set of equations of motion for a group of components which are not connected. A set of relationships exists which corresponds physically to connecting the components to form a system. These relationships result from requirements that displacements at mutual attachment points must be equal. This corresponds to a

transformation relating the component coordinates to the system coordinates. The details of the transformation depend on the system being analyzed.

This same discussion applies in a similar manner to normal modes of components. The motions of one component may be expressed in terms of its normal modes while the motions of a second component may be determined in terms of its normal modes. The normal modes of the combined system may be determined in terms of the component modes by satisfying the requirements for compatibility of displacements at the attachment points between the two components.

This method would be useful, for instance, for determining the natural modes and frequencies of a launch vehicle with several different payload configurations. The natural modes of the vehicle could be computed for the vehicle without the payload and for the payload alone; the combined system could then be determined in terms of these modes for each payload configuration.

The method offers the advantage of being able to combine analytically determined modal data with experimentally determined modal data where available. For large structures, modes of individual portions may be determined by test, while tests of the entire structure may not be practical.

3.3 CORRECTING MODEL BASED ON TEST RESULTS

The final evaluation of analytical techniques is a comparison with experimental data. Perfect comparisons are indeed exceptions, since both the analytical model and experimental model are approximations to some extent. The analytical approximations have been discussed. The major experimental approximations are centered around suspension system effects and vehicle modifications required to accommodate the suspension system. No general rule can be made to obtain better agreement between test and analysis. Careful examination of the data and the structure will probably indicate several areas where the representation is inadequate or does not define the test specimen. Possible causes of differences are:

a. Effects of suspension system on test environment.

b. Stiffness of joints or trusses.

c. Assumed planes of symmetry are incorrect.

d. Effect of large components such as engines.

e. Experimental modes may be impure, i.e., not orthogonal.

f. Effects of moment of inertia.

g. Nonlinearity.

The work of Reference 14 presents a method for obtaining the flexibility matrix from experimental mode data. The procedure orthogonalizes the experimental modes, using an analytical mass distribution, and then derives the flexibility matrix of the structure. This method can be useful if complete and accurate experimental data are obtained for a system difficult to model. It can also be used to locate possible discrepancies between analytical and experimental results.

3.4 SOLID-PROPELLANT BOOSTERS

The structural dynamics of solid propellant rockets have generally been treated by continuous representations, for instance as in Reference 7. The effective longitudinal stiffness of the core depends primarily on the shear stiffness of the solid propellant. Inertial forces acting on the core material are transmitted to the rocket casing through shear stresses developed in the core material. An element of a solid-propellant rocket is shown in Figure 23.

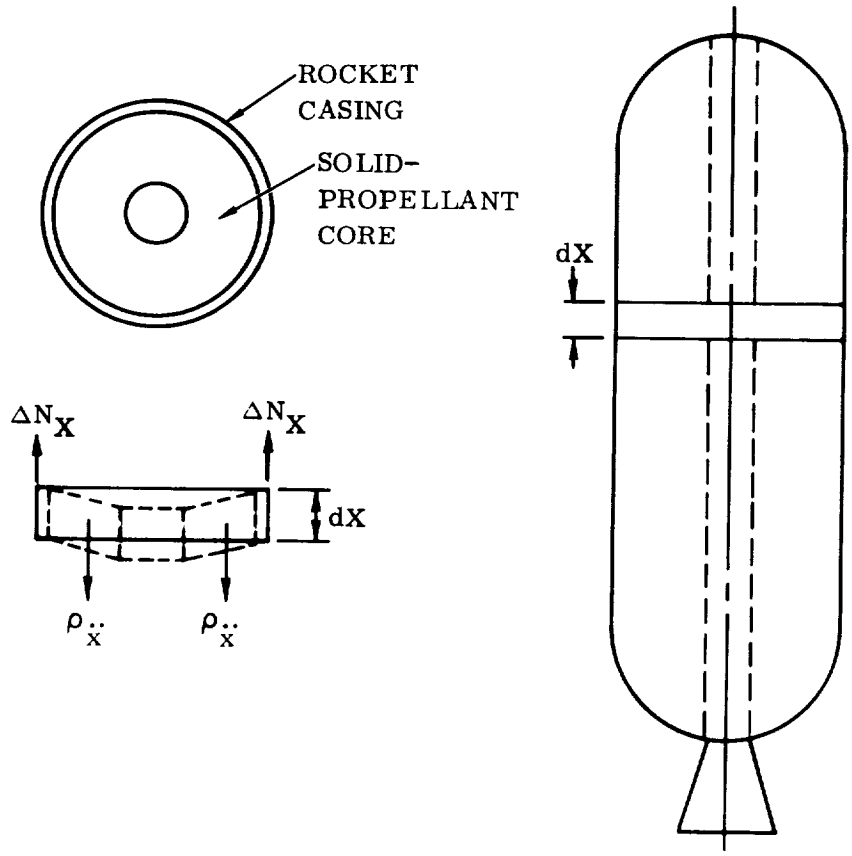

Figure 23. Solid-Propellant Rocket Element

The inertial forces $\rho \ddot{x}$ acting on the core cause shearing of the core relative to the casing and produce an increment of axial force in the casing, ΔN_X, over the length dX. The shear deformation is indicated under axial acceleration of the element. A simple model for the solid-propellant rocket could be obtained by integrating the effects of axisymmetric shear deformations of the propellant and axial deformations of the casings. The propellant may be relatively more flexible than the casing; the casing might then be assumed rigid.

Reference 7 provides a more detailed analysis of the structural dynamics of a solid-propellant rocket; included are stress-strain laws for solid-propellant materials. Several problems are considered using a continuous representation of the solid-propellant rocket.

Once a model for the solid-propellant rocket is obtained, the remainder of the vehicle can be modeled in the same manner as for a liquid-propellant vehicle.

3.5 CLUSTERED BOOSTERS

One method for obtaining the higher thrust required for large payloads is to attach rocket engines or motors to a central core; for liquid-propellant boosters a peripheral ring of propellant tanks is attached to a central tank and the engines are supported on truss members connecting the tanks; for solid-propellant boosters, the motors are attached to a central solid- or liquid-propellant booster. These clustered tank designs destroy axial symmetry and quite often planes of symmetry. Such configurations result in a more complicated dynamic model where a number of cylindrical tanks are coupled by their elastic connections and must be allowed freedom in several directions for adequate description of vehicle modes (see Figure 24).

For preliminary design it is sufficient to choose approximate planes of symmetry and analyze the vehicle for bending modes in pitch and yaw planes using branch beams connected to the central core by translational and rotational springs. Simplified torsional and longitudinal models will also suffice at this stage. These simple models can be used to identify possible problem areas (such as relative modal frequencies) and provide design criteria for the connections between tanks.

A complete analysis (or carefully conducted test) should be undertaken to describe all the primary modes of the clustered vehicle. This analysis would provide translation and rotation in two mutually perpendicular planes; torsion and longitudinal motion. The model of the tanks for translation and rotation in each of the two planes would be very similar to that discussed for the cylindrical booster. Provision must be made to account for the motion of the outer tanks in these two directions due to the torsional displacement of the central tank and the elastic connections. It is also possible that

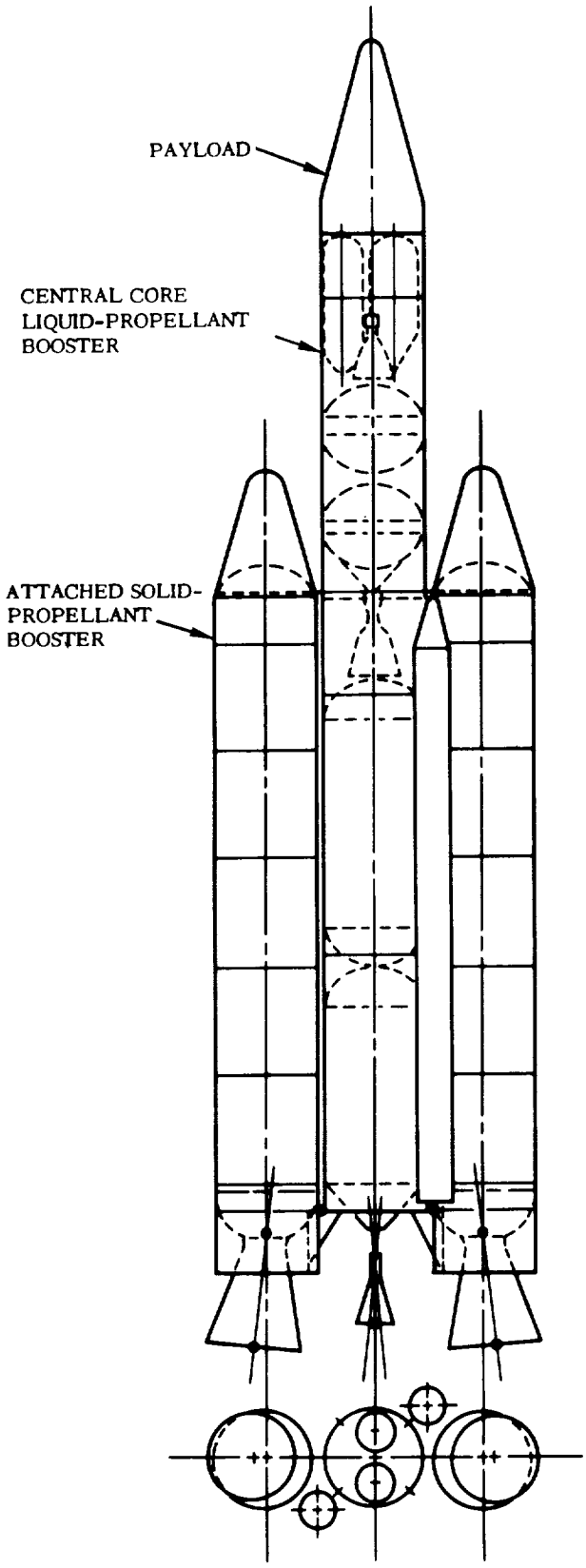

Figure 24. Titan IIIC

longitudinal motion will couple with lateral and torsional displacement. As an example, consider a cluster arrangement where the connection at the bottom provides moment, shear, and axial restraints while the connection at the top provides only shear restraint. Then it is possible to find a mode where the external tanks are bending, causing moments and deflections at the connection to the center core which will result in longitudinal motion of the core. The significance of these types of modes can be ascertained only from the analysis (or test) and can vary greatly from vehicle to vehicle.

The torsional properties in the model can be represented by the torsional stiffness and roll inertia of each tank. The tanks must then be connected by the elastic properties of the truss. The complete model for the clustered booster then consists of the axial load, shear, bending moment, and torque. The top connection transmits only shear. Because of the nature of the connections, it can be seen that yaw bending and longitudinal coupling can occur. Pitch bending and torsion represent another possible coupling mechanism. Storey in Reference 14 develops the coupled flexibility matrices for these two conditions. This method encountered difficulty in that the number of stations required for adequate representation of the system with the required transformations exceeded computer capacity.

The final Titan IIIC analysis presented in Reference 15 utilizes the mode synthesis approach. The longitudinal, torsional, and pitch and yaw bending modes are determined for each tank and are then coupled by the elasticity of the connecting elements. The influence coefficients for these trusses were obtained experimentally. A comparison of analytical and 1/5-scale experimental results is given in Reference 17.

3.6 LATERAL-TORSIONAL-LONGITUDINAL COUPLING

The typical axisymmetric-cylindrical space vehicle is analyzed as if lateral, torsional, and longitudinal motion are not coupled. Actually, these vehicles are not completely symmetric and a possible coupling mechanism, however slight, can always be found. The importance of this coupling can vary greatly from vehicle to vehicle and even if it is known to exist from flight or experimental data, the coupling mechanism is difficult to identify. These coupling problems often occur when the modal frequencies of two modes, say, one lateral and one torsional, are very close together. Then a very small coupling mechanism, such as center-of-gravity offset from the supposed line of symmetry, can result in coupled motion.

A comparison of the frequencies of the modes in the three directions should be made to determine the existence of modes of nearly equal frequency. If such a condition exists, it is necessary to examine the condition under which this may cause a significant problem. As an example, if excitation of a bending mode by an atmospheric disturbance occurred, could this cause excitation of a critical torsional mode at this same frequency?

Cylindrical vehicles with unsymmetric upper stages or payloads of large mass can cause coupling in the various directions in the low-frequency modes. The model and analysis then become complicated and approach that of the clustered boosters. Representation of this configuration requires detailed description in the unsymmetric stages and an analysis as described later for clustered boosters. Preliminary work would indicate the degree of sophistication to be used for adequate representation for loads analysis.

The Saturn I vehicle consists of a center LO_2 tank with eight peripheral tanks for alternating LO_2 and RP-1. These tanks are connected at top and bottom by trusses providing axial, shear, and torsion restraint in both planes at the bottom plus moment restraint in the tangential planes. The top connection provides similar restraint except for the fuel tanks which do not transmit axial load. The trusses are not symmetric with respect to planes of symmetry of the tanks, but this effect is small so that planes of symmetry as defined by the tanks do not introduce large errors.

Milner (Reference 18) establishes theoretically the uncoupling of pitch, yaw, and torsion modes for a symmetrical cluster booster and investigates the effect of minor asymmetry. Results of this study indicate that the effect of such coupling on natural frequencies is minor; mode shapes are not presented.

Lianis (Reference 19) develops a matrix solution of the dynamics problem of a four-tank booster without center core. The flexibility matrix of the whole unit, with appropriate beam end fixity, is derived. This flexibility matrix together with a suitable mass matrix is used to derive equations of free vibration in matrix form. The tanks are assumed to be similar, but the solution can be modified accordingly for the

case of nonsimilar tanks and for other tank configurations. The formulation is general so as to furnish any complex mode of vibration. Simple modes, however, can be obtained as particular cases of the general problem.

3.7 DAMPING EFFECTS

Dissipative (damping) forces exist in the vibrating structure as a result of material strain hysteresis and coulomb friction in structural joints. The nature of these damping effects is obscure and does not lend itself to analysis other than an approximate empirical treatment, by which the gross effect of these scattered dissipative mechanisms is represented as equivalent viscous damping, added to each mode as appropriate. The damping is thus assumed to produce no coupling between modes. While this mechanization is not entirely realistic, it is justified by two observations: First, the actual damping is very low and is found by test to produce little coupling. Thus nearly pure normal modes of a system may be excited and the system observed to decay almost harmonically. The indication given is that velocity-dependent coupling is very small. Second, if an attempt is made to show a velocity-dependent coupling, the coefficient would have to be determined experimentally. Since the direct damping coefficient is itself difficult enough to measure it is clear that the accuracy of a study cannot be increased by the introduction of still more suspect data. The structural damping force is a function of the deflection of the generalized coordinate of the mode but in phase with the velocity of the generalized coordinate of that mode. To treat this damping as viscous damping requires that the mode oscillate in a quasi-harmonic manner. This damping force may then be expressed as a damping factor, ζ_n, where $2\zeta_n\omega_n\dot{\xi}_n$ is the internal damping force of the n^{th} mode per unit generalized mass.

Fluid propellant damping forces result from the dissipative nature of a viscous fluid undergoing shear. Although there are some approximate methods for calculating damping forces, these forces are most commonly arrived at by testing the actual tank, in the case of small vehicles, and a model tank in the case of large vehicles. These forces may be represented as a propellant damping factor, ζ_n, in the expression $2\zeta_n\omega_n\dot{\xi}_n$ which is the damping force per unit sloshing mass and $\dot{\xi}_n$ is the lateral velocity of the n^{th} sloshing mass.

Aerodynamic damping forces result from lateral velocity of the vehicle which causes, for any particular point on the vehicle, a small angle of attack. The aerodynamic force associated with this angle of attack opposes the lateral motion, thereby dissipating energy. The aerodynamic damping forces are easily calculated and are, of course, a function of $\dot{\xi}_n$. Aerodynamic damping on launch vehicles is often not important for dynamic load analyses; however, for some configurations, e.g., hammerhead payloads and winged payloads, it may need to be considered.

4/METHODS FOR SOLUTION

4.1 FORMATION OF THE EQUATIONS FOR SOLUTION

The longitudinal model provides a mathematical representation of the real physical system. As outlined in Section 3, dynamic characteristics of the model are determined from the mass, stiffness, and dynamic matrices.

4.1.1 STIFFNESS MATRIX. Formation of the dynamic matrix for computation of modal properties requires formation of the mass and flexibility matrices. The flexibility matrix is not ordinarily formed directly but is usually obtained by inversion of the stiffness matrix. (See the Reference 8 matrix inversion methods.) This procedure is followed since the stiffness matrix can generally be formed in a simpler and more direct manner than the flexibility matrix (see Reference 6).

Where spring-mass models are employed, the relationship between spring constants and the stiffness matrix is fairly simple. The stiffness matrix element K_{ij} is the force at i due to a unit displacement at j only with all other displacements equal to zero. Off-diagonal elements K_{ij} of the stiffness matrix are simply the negative value of the stiffness of the spring connecting node i to the node j of the model. The diagonal element K_{ii} of the stiffness matrix represents the sum of the stiffnesses of all springs connected to node i. As an example, consider the spring-mass model of Figure 25.

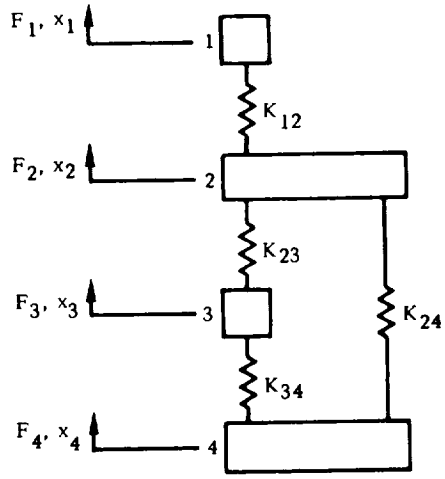

Figure 25. Spring-Mass Model

The stiffness matrix for the model relates forces to displacements as follows.

$$\begin{Bmatrix} F_1 \\ F_2 \\ F_3 \\ F_4 \end{Bmatrix} = \left[\begin{array}{c|c|c|c} K_{12} & -K_{12} & 0 & 0 \\ -K_{12} & K_{12}+K_{23}+K_{24} & -K_{23} & -K_{24} \\ 0 & -K_{23} & K_{23}+K_{34} & -K_{34} \\ 0 & -K_{24} & -K_{34} & K_{24}+K_{34} \end{array}\right] \begin{Bmatrix} x_1 \\ x_2 \\ x_3 \\ x_4 \end{Bmatrix} \quad (117)$$

Note that the coefficients in column one are forces due to a unit displacement at node 1 only with displacements at 2, 3, and 4 of zero. The force required to produce the unit displacement at node 1 is K_{12} while $-K_{12}$ is the reaction at 2 corresponding to the unit displacement at 1.

If the following stiffness matrix is for absolute displacements of a free structure,

$$[K] = \begin{bmatrix} K_{11} & K_{12} & K_{13} \\ K_{21} & K_{22} & K_{23} \\ K_{31} & K_{32} & K_{33} \end{bmatrix} \tag{118}$$

and the associated mass matrix is a diagonal matrix, the corresponding model and springs are

$$\left.\begin{aligned} K_{12} &= -K_{12} \\ K_{13} &= -K_{13} \\ K_{23} &= -K_{23} \end{aligned}\right\} \tag{119}$$

where the model is given in Figure 26.

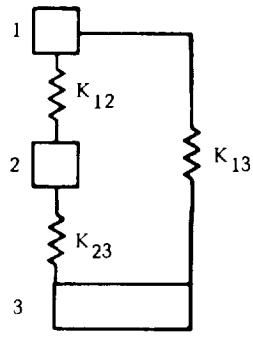

Figure 26. Model Corresponding to Stiffness Matrix

The methods for deriving stiffness matrices or spring-mass models for propellant tanks and other portions of the structure were discussed in Section 3. Assembly of the vehicle stiffness matrix is accomplished by superposing or adding the stiffness matrices of the individual elements.

One of the problems of obtaining a solution to the equations of motion for a free-free structure with no external forces applied is that the stiffness matrix of such a structure is singular. The structure could move as a rigid body upon application of any external force. In this instance inverting the stiffness matrix to obtain a flexibility matrix may not be done directly. Several methods are available to overcome this difficulty. They are essentially the use of an additional equation, which states that for free vibration of a free-free structure the summation of the inertial forces is zero:

$$-\omega^2 \sum_{i=1}^{m} m_i x_i = 0 \tag{120}$$

From this equation we may choose an arbitrary mass, say m_1, and let

$$m_1 x_1 = -\sum_{i=2}^{m} m_i x_i \tag{121}$$

therefore

$$x_1 = -m_1^{-1} \sum_{i=2}^{m} m_i x_i \tag{122}$$

Then in matrix notation,

$$x_1 = -m_1^{-1} \langle m_2 m_3 \cdots\cdots m_m \rangle \{x'\}$$

$$= \langle E \rangle \{x'\} \tag{123}$$

$$\{x\} = \begin{Bmatrix} x_1 \\ \hline x' \end{Bmatrix} \tag{124}$$

Then

$$\{x\} = \begin{bmatrix} E \\ \hline I \end{bmatrix} \{x'\} \tag{125}$$

Then from Equation 12, page 7, with the stiffness given by

$$[K] = \left[\begin{array}{c|c} \alpha & \gamma^T \\ \hline \gamma & \beta \end{array}\right] , \tag{126}$$

$$-\omega^2 \left[\begin{array}{c|c} m_1 & 0 \\ \hline 0 & m' \end{array}\right] \left[\begin{array}{c} E \\ \hline I \end{array}\right] \{x'\} + \left[\begin{array}{c|c} \alpha & \gamma^T \\ \hline \gamma & \beta \end{array}\right] \left\{\begin{array}{c} E \\ \hline I \end{array}\right\} \{x'\} = 0 \tag{127}$$

Expanding the second equation,

$$-\omega^2 [m'] \{x\} + \Big[\{\gamma\} \langle E \rangle + [\beta]\Big] \{x'\} = 0 \tag{128}$$

Therefore

$$[K'] = \{\gamma\} \langle E \rangle + [\beta] \tag{129}$$

and

$$\frac{1}{\omega^2}\{x'\} = [K']^{-1}[m']\{x'\} \tag{130}$$

The above equation may be used to solve for the natural modes and frequencies of the free structure. Once x' has been determined, x_1 may be determined from Equation 123.

4.1.2 FLEXIBILITY MATRIX. The flexibility matrix may be developed directly for simple statically determinant structures by determining the displacements due to unit loads. However, obtaining the stiffness matrix and inverting it is easier when very many redundancies exist in the structure. For direct development of the flexibility matrix in terms of the flexibility matrices of individual structural elements for complex structures, see Reference 20.

4.1.3 TRANSFORMED MASS MATRIX. An approach that is particularly advantageous for close-coupled systems is that of transforming the coordinate system from the absolute to the relative sense. In prior discussions the displacements of the system coordinates have been referenced to a fixed point or neutral position. These same displacements may also be expressed relatively; referenced to an adjacent coordinate. The relationship between displacements in absolute terms, $\{x\}$, and the displacements in relative terms, $\{\bar{x}\}$, is readily described by a simple transformation matrix:

$$\{x\} = [T]\{\bar{x}\} \tag{131}$$

Thus the kinetic energy of the system can be expressed in terms of relative coordinates by

$$2\,KE = \{\dot{\bar{x}}\}'[T]'[M][T]\{\dot{\bar{x}}\} \tag{132}$$

The deflections of the connecting springs are expressed in terms of relative coordinates, which in its most general form requires another transformation matrix.

$$\{\Delta\} = [TR]\{\bar{x}\} \tag{133}$$

If the number of springs is equal to or less than the number of inertias, the deflection of each spring will be defined by a different relative displacement; consequently the transformation matrix, $[TR]$, can be written as a diagonal matrix of unit elements. For such a case, $[TR]$ may be neglected without affecting the solution.

The potential energy of the system is given by

$$2\,PE = \{\bar{x}\}'[TR]'[K][TR]\{\bar{x}\} \tag{134}$$

where K is a diagonal matrix of the spring rates.

Substituting the kinetic energy and potential energy terms into LaGrange's equation

$$\frac{d}{dt}\left[\frac{\partial(KE)}{\partial \dot{q}_i}\right] + \frac{\partial PE}{\partial q_i} + \frac{\partial W}{\partial q_i} = 0 \tag{135}$$

the equations of motion become

$$[T]'\,[M]\,[T]\,\{\ddot{\bar{x}}\} + [TR]'\,[K]\,[TR]\,\{\bar{x}\} = 0 \tag{136}$$

and the dynamic matrix is established by

$$\left[\left([TR]'\,[K]\,[TR]\right)^{-1}\,[T]'\,[M]\,[T]\right]\,\{\phi\} = \lambda\,\{\phi\} \tag{137}$$

The advantages of this method are greatest when the system is free or cantilevered and multiple load paths are absent or constitute only a minor portion of the system. Under these conditions, the transform matrix [TR] contains little or no off-diagonal terms; the matrix $[TR]'\,[K]\,[TR]$ is no more than slightly coupled and may be inverted with a minimum of effort.

When the number of springs is equal to or less than the number of inertias, the transform matrix is a diagonal matrix of unit elements; $[TR]'\,[K]\,[TR]$ reduces to [K] which, being a diagonal matrix, can be immediately inverted by taking the reciprocals of the individual elements of the diagonal. The dynamic matrix can be determined with a minimum of effort and operated on to obtain modal data.

4.2 SOLUTION FOR CHARACTERISTICS

After the stiffness and mass matrices for the model are formed, the equations of motion may be written with external forces equal to zero. This set of linear differential equations may be solved for modal properties by several techniques. If the equations for harmonic motion,

$$-\omega^2\,[M]\,\{x\} + [K]\,\{x\} = 0 \tag{138}$$

are written in the form

$$\left[[K] - \omega^2\,[M]\right]\,\{x\} = 0 \tag{139}$$

then for

$$\{x\} \neq 0$$

a solution exists only if the determinant

$$\left|[K] - \omega^2 [M]\right| = 0 \tag{140}$$

Expansion of the above determinant leads to a polynomial. If [K] and [M] are n^{th} order matrices, the polynomial (characteristic equation) will be n^{th} order and have n roots. The roots of the polynomial yield the natural frequencies ω. Particular natural frequencies may be inserted in Equation 139 to determine the corresponding natural mode shape. This procedure results in determination of all natural frequencies and mode shapes. The method is very useful for small matrices but becomes difficult to use for large matrices. Since only lower frequency modes are generally of importance, other methods are usually used which do not require direct solution for the roots of the characteristic equation. Among these methods are the matrix iteration, Holtzer (Myklestad), and energy (Rayleigh-Ritz) methods. Matrix iteration is discussed in References 8 and 21; the Holzer (Myklestad) method and the Rayleigh-Ritz method are discussed in References 21 and 22.

4.3 MODAL SYNTHESIS

If a structural model requires a very large number of degrees of freedom, computation of modal properties of the entire structure directly may pose a difficult problem. The structure could be divided into several parts and the modal properties could be computed for several modes of each part. The dynamic properties of the entire structure could then be determined from the properties of the parts using the method of modal synthesis. This method is discussed in detail in References 13, 21, and 23.

5/REFERENCES

1. L. L. Fontenot and G. Lianis, "The Free Vibrations of Thin Elastic Pressurized Cylindrical Shells with a Free and Incompressible Liquid Having a Free Surface," International Symposium on Space Technology and Science, Paper No. 6-6-8, 1963.

2. J. D. Wood, Survey on Missile Structural Dynamics, Report 7102-0041-NU-000, Contract No. AF 04(647)-619, 1 June 1961.

3. R. G. Rose, J. A. Staley, and A. K. Simson, A Study of System-Coupled Longitudinal Instabilities in Liquid Rockets, Report AFRPL-TR-65-163, Contract AF 04(611)-9956, September 1965.

4. L. D. Pinson, Longitudinal Spring Constants for Liquid-Propellant Tanks with Ellipsoidal Ends, NASA Technical Note D-2220, November 1964.

5. J. S. Archer and C. P. Rubin, Improved Analytic Longitudinal Response Analysis for Axisymmetric Launch Vehicles, NASA CR-345, Contract NAS1-4351, December 1965.

6. M. J. Turner, R. W. Clough, H. C. Martin, and L. J. Topp, "Stiffness and Deflection Analysis of Complex Structures," Journal of the Aeronautical Sciences, Vol. 23, No. 9, September 1956.

7. J. H. Baltrukonis, A Survey of Structural Dynamics of Solid Propellant Rocket Motors, NASA Report NASA CR-658, December 1966.

8. V. N. Faddeeva, Computational Methods in Linear Algebra, Dover Publications, New York, 1959.

9. S. Timoshenko, Theory of Plates and Shells, McGraw-Hill Book Company, Inc., First Edition, 1940.

10. R. G. Rose, Dynamics of the Atlas 5-CPS Longitudinal Oscillation Following Launch as Related to the Tank Pressure Regulation System, Convair Division Report GDA63-0712, Volumes I and II, Contracts AF 04(694)-196 and AF 04(695)-240.

11. L. D. Pinson, H. W. Leonard, and J. P. Ramey, "Analysis of Longitudinal Dynamics of Launch Vehicles with Application to a 1/10-Scale Saturn V Model," AIAA/ASME 8th Structures, Structural Dynamics, and Materials Conference, Palm Springs, March 1967.

12. R. H. Schuett, B. A. Appleby, J. D. Martin, Dynamic Loads Analysis of Space Vehicle Systems, Launch and Exit Phase, Convair division of General Dynamics Report GDC-DDE66-012, June 1966.

13. W. C. Hurty, Dynamic Analysis of Structural Systems by Component Mode Synthesis, TR 32-530, Jet Propulsion Laboratory, Pasadena, California, January 1964.

14. S. I. Gravitz, "An Analytical Procedure for Orthogonalization of Experimentally Measured Modes," Journal of the Aerospace Sciences, November 1958.

15. R. E. Storey, "Dynamic Analysis of Clustered Boosters with Application to Titan III," AIAA 1963 Summer Meeting, Paper No. 63-208, June 1963.

16. Bodley, Ikard, and Schulta, Vibration Analysis Report, Program 624A, Configuration C, Flight Plan VIII, Air Force Report No. SSD-CR-65-1, January 1965.

17. I. J. Jaszlics, Program 624A 20%-Scale Dynamic Model Ground Vibration Survey, Final Test Report, Vol. III, SSD-CR-65-47, Martin Company, Denver, Colorado, May 1965.

18. J. L. Milner, Three Dimensional Multiple Beam Analysis of a Saturn 1 Vehicle, NASA TMX-53098, July 1964.

19. G. Lianis, Matrix Analysis of Vibrations of Clustered Boosters, Convair Division Report AE61-0858, September 1961.

20. E. C. Pestal and F. A. Leckie, Matrix Methods in Elastomechanics, McGraw-Hill, 1963.

21. A Monograph on Lateral Vibration Modes, Convair Report GDC-DDF65-001, Contract NAS8-11486, 22 February 1965.

22. L. S. Jacobsen and R. S. Ayre, Engineering Vibrations, McGraw-Hill, 1958.

23. A Monograph on Torsional Vibration Modes, Convair Report GDC-DDF65-003, Contract NAS8-11486, 3 May 1965.

"The aeronautical ...
conducted so as to ...
... of phenomena ...
... provide for the ...
... of information concerning ...

NASA SCIENTIFIC A... ...ATIONS

...ICAL REPORTS: ... ...d, ... complete, and ...

...IC NOTES: ... ... of ... ... a contribution ...

...ICAL MEMORAN... ... ... preliminary ...

CONTRACTOR REPORTS: ... ...d ... under a NASA contract or ... ... to ... existing knowledge.

TECHNICAL TRANSLATI... ... ... considered to merit NA...

SPECIAL PUBLICATIONS: ... ... activities. Publications ... ... compilations, handbooks, ...

TECHNOLOGY UTILIZATI... ... ... pology used by NASA that ... ... non-aerospace applications. ... Publication Reports and Notes, ...

Copies of the ... available ...

... SCIENTIFIC AND ...

NATI... AERONAU... ...ATION